UNCLASSIFIED

AD NUMBER

AD864392

LIMITATION CHANGES

TO:

Approved for public release; distribution is unlimited.

FROM:

**Distribution authorized to U.S. Gov't. agencies and their contractors;
Administrative/Operational Use; JAN 1970. Other requests shall be referred to Arnold Engineering Development Center, Arnold AFB, TN.**

AUTHORITY

AEDC ltr 7 Aug 1973

THIS PAGE IS UNCLASSIFIED

ARCHIVE COPY
DO NOT LOAN

AEDC-TR-69-268

cy1

HIGH MACH NUMBER, HIGH REYNOLDS NUMBER PERFECT GAS WIND TUNNELS, AND A METHOD OF PERFORMANCE COMPARISON

A. H. Boudreau, Jr.

ARO, Inc.

This document has been approved for public release ... its distribution is unlimited.

Per A. J. Letter dtd 7 Aug. 73 Signed William O. Cole

January 1970

This document is subject to special export controls and each transmittal to foreign governments or foreign nationals may be made only with prior approval of Arnold Engineering Development Center (AETS), Arnold Air Force Station, Tennessee 37389.

VON KÁRMÁN GAS DYNAMICS FACILITY
ARNOLD ENGINEERING DEVELOPMENT CENTER
AIR FORCE SYSTEMS COMMAND
ARNOLD AIR FORCE STATION, TENNESSEE

PROPERTY OF U. S. AIR FORCE
AEDC LIBRARY
F40600 - 69 - C - 0001

AEDC TECHNICAL LIBRARY
5 0720 00032 7686

NOTICES

When U. S. Government drawings specifications, or other data are used for any purpose other than a definitely related Government procurement operation, the Government thereby incurs no responsibility nor any obligation whatsoever, and the fact that the Government may have formulated, furnished, or in any way supplied the said drawings, specifications, or other data, is not to be regarded by implication or otherwise, or in any manner licensing the holder or any other person or corporation, or conveying any rights or permission to manufacture, use, or sell any patented invention that may in any way be related thereto.

Qualified users may obtain copies of this report from the Defense Documentation Center.

References to named commercial products in this report are not to be considered in any sense as an endorsement of the product by the United States Air Force or the Government.

HIGH MACH NUMBER, HIGH REYNOLDS NUMBER PERFECT GAS WIND TUNNELS, AND A METHOD OF PERFORMANCE COMPARISON

A. H. Boudreau, Jr.
ARO, Inc.

This document has been approved for public release and its distribution is unlimited. Per A.F. Letter dated Jan. 73. signed William O. Cole.

~~This document is subject to special export controls and each transmittal to foreign governments or foreign nationals may be made only with prior approval of Arnold Engineering Development Center (AETS), Arnold Air Force Station, Tennessee 37389.~~

FOREWORD

The research reported herein was sponsored by the Arnold Engineering Development Center (AEDC), Air Force Systems Command (AFSC), Arnold Air Force Station, Tennessee, under Program Element 65401F/876/6226.

The results of research were obtained by ARO, Inc. (a subsidiary of Sverdrup & Parcel and Associates, Inc.), contract operator of AEDC, AFSC, under Contract F40600-69-C-0001. The research was performed from May 5 to July 15, 1969, under ARO Project No. VT8002, and the manuscript was submitted for publication on November 4, 1969.

This report was originally prepared as a thesis for the University of Tennessee Space Institute in partial fulfillment for the Master of Science degree.

Information in this report is embargoed under the Department of State International Traffic in Arms Regulations. This report may be released to foreign governments by departments or agencies of the U. S. Government subject to approval of the Arnold Engineering Development Center (AETS), or higher authority within the Department of the Air Force. Private individuals or firms require a Department of State export license.

This technical report has been reviewed and is approved.

Eugene C. Fletcher	Roy R. Croy, Jr.
Lt Col, USAF	Colonel, USAF
AF Representative, VKF	Director of Test
Directorate of Test	

ABSTRACT

The regimes of high velocity flight are investigated and simulation of such conditions is shown to require simulation of high Reynolds numbers in addition to high Mach numbers, plus consideration of thermo-chemical-kinetic effects. Real gas simulation, which requires duplication of stagnation enthalpy is shown to be impractical in wind tunnels. Perfect gas simulation is, however, shown to offer an alternative means of high velocity simulation. Considerations of perfect gas simulation are discussed which include non-equilibrium of the test gas, source flow considerations, and saturation limits. A method of comparing perfect gas wind tunnels is then developed based on the basic fluid dynamics scaling parameters plus considerations of reservoir pressure limits and decay rates, wind tunnel size, saturation temperature limits, viscosity considerations, and nitrogen as a test gas. Computer calculations of real gas air and nitrogen expansions for unit Reynolds number are presented graphically based on the method developed for comparing facilities. Finally, four perfect gas wind tunnel facilities which represent the present state of the art are compared using the developed technique.

This document is subject to special export controls and each transmittal to foreign governments or foreign nationals may be made only with prior approval of Arnold Engineering Development Center (AETS), Arnold Air Force Station, Tennessee 37389.

This document has been approved for public release; its distribution is unlimited.

per A.F. Letter dated 7 Aug 73
Signed William O. Cole

CONTENTS

ILLUSTRATIONS

Figure

TABLES

NOMENCLATURE

a_∞	Speed of sound
A	Reference area
C_D	Drag coefficient
C_p	Specific heat at constant pressure
d*	Wind tunnel throat diameter
g	Acceleration due to gravity
h_∞	Free stream enthalpy
H_o	Total or stagnation enthalpy
K_1	Constant in the viscosity equations (equations 15 and 16)
K_2	Constant in the viscosity equations (equations 15 and 16)
Kn	Knudsen number
K_∞	Free stream thermal conductivity
ℓ	Characteristic length
M_∞	Free stream Mach number
P	Pressure
P_E	Newtonian pressure on a model in source flow
P_o	Reservoir pressure
$P_{o\ max}$	Maximum reservoir pressure
Pr	Prandtl number
P_∞	Free stream pressure
q_∞	Free stream dynamic pressure
r	Radial distance from a wind tunnel centerline to a point in the flow field

r_m	Radial distance from a wind tunnel centerline to a point on a model
r_N	Radial distance from a wind tunnel centerline to the nozzle wall
R	Gas constant
Re_∞	Free stream Reynolds number
Re/ft	Reynolds number based on free stream conditions and a one foot length
Re_{∞_D}	Reynolds number based on free stream conditions and wind tunnel core diameter
Re_{∞_ℓ}	Reynolds number based on free stream conditions and a characteristic length
Re_{∞_x}	Reynolds number based on free stream conditions and distance along the wind tunnel nozzle centerline from the throat
S/R	Dimensionless entropy
t	Time
T	Temperature
T_o	Reservoir temperature
$T_{o_{max}}$	Maximum reservoir temperature
T_w	Wall temperature
T_∞	Free stream temperature
U_∞	Free stream flow velocity
V	Volume
W	Weight
x	Distance along the nozzle centerline measured from the throat

β	Shock angle
γ	Ratio of specific heats
δ	Boundary layer thickness
ΔE	Change in energy
ΔM	Change in Mach number
ΔP	Change in pressure
θ_C	Cone half angle
θ_N	Nozzle half angle
λ	Molecular mean free path
μ	Free stream viscosity
ρ	Density
ρ_o	Sea level density
ρ_∞	Free stream density

SECTION I
INTRODUCTION

The performance of modern aerospace systems has greatly expanded the altitude-velocity envelope to be duplicated in ground test facilities. The present Apollo program encompasses the entire altitude-velocity range of current ground test facilities and requires the simulation of velocities as high as 37,000 feet per second at relatively low altitudes (200,000 feet). Most advanced wind tunnel facilities are today operated at their maximum performance limits in an attempt to adequately simulate such high velocity flight conditions. Many test facilities of various types are presently being developed to further extend our present performance limits. This report will examine the regimes of high velocity flight and develop a method of making comparisons among one type of advanced wind tunnel facility for high velocity flight simulation.

Figure 1 shows the extent of present day interest in high velocity flight, as defined by Korkegi, Kubota, and Mickey (1)[1]. The flight envelope described in Figure 1 contains a corridor of continuous flight, ballistic re-entry trajectories, and a lunar re-entry trajectory. Both continuous flight and re-entry trajectories indicate a definite need for adequate simulation in the high velocity (high Mach number)

---

[1]Numbers in parentheses refer to similarly numbered references in the bibliography.

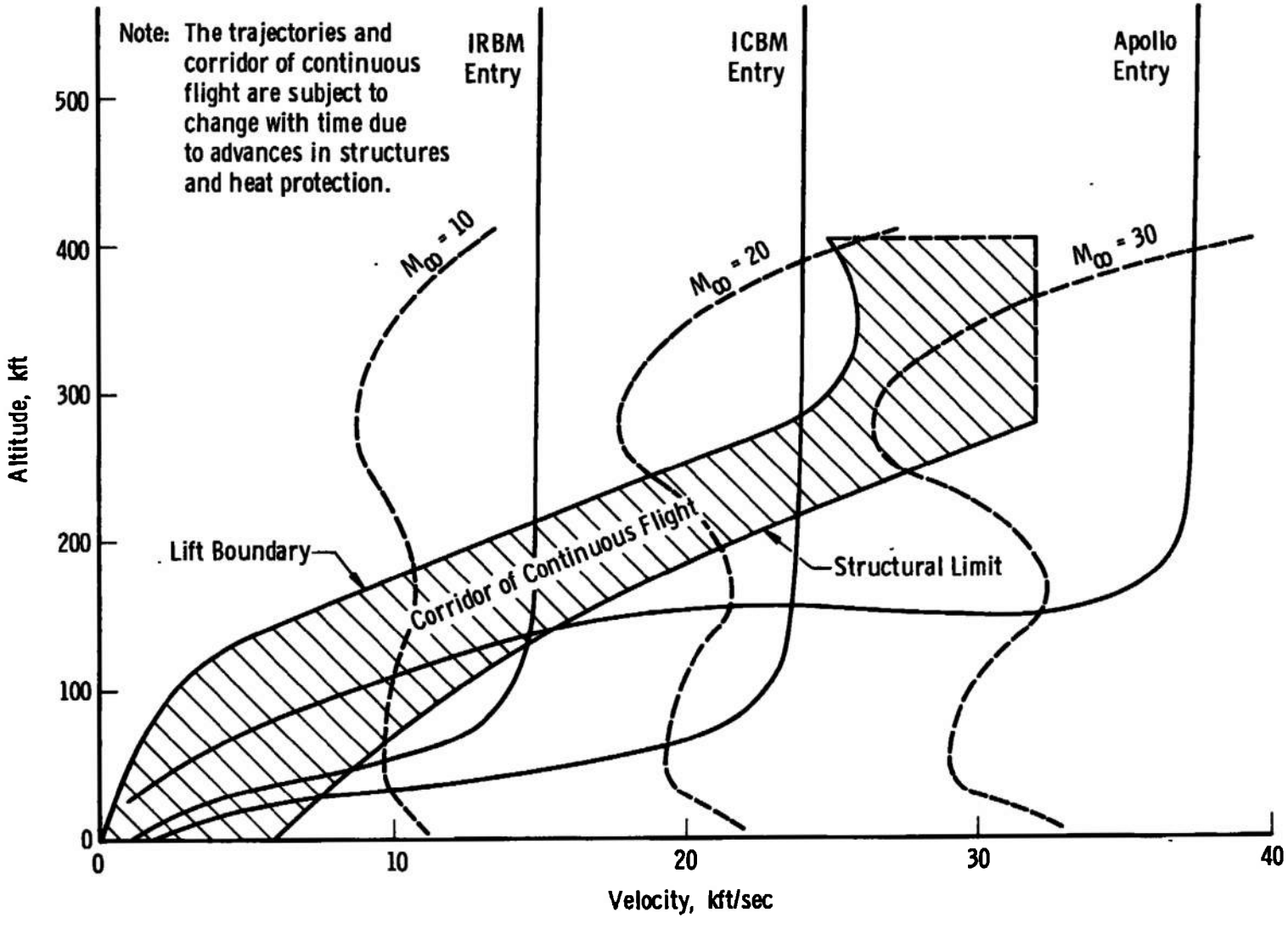

Figure 1. High velocity flight regimes.

regime. Post lunar missions indicate future interest in velocities in excess of 40,000 feet per second. Note that ballistic missiles maintain Mach 20 to altitudes as low as 80,000 feet. Conceptual reuseable launch vehicles utilizing Scramjet propulsion systems will fly the entire continuous flight corridor to deliver payloads to high altitudes at near orbital velocities. Small rocket propulsion units would then complete insertion of the payload into orbit. This flight corridor consists of the altitude-velocity plane between an upper limit at which sufficient lift can no longer be generated to support the vehicle, and a lower limit at which aerodynamic and thermodynamic loads become excessive. The lower limit on all trajectories of Figure 1 can be lowered with future advances in structures and heat protection.

In the hypersonic aerodynamic flight regime being considered here, both the purely fluid dynamic effects arising from high Mach numbers and the thermo-chemical-kinetic effects (often called 'real gas effects') interact in a complex fashion to determine the aerodynamics of the vehicle. Flight environments such as these place stringent requirements on ground test facilities, for implicit in the trajectories of Figure 1 is the very difficult requirement of high Reynolds numbers being simulated along with high Mach numbers. The Reynolds number is one of the basic aerodynamic simulation parameters and characterizes the relationship between a characteristic dimension on a vehicle and the flow properties of velocity, density, and viscosity. It qualitatively may be expressed as the relationship of inertial to viscous forces. Hence the flow field about a body in this high Reynolds number regime will exhibit

large inertial, or pressure forces, compared to viscous forces. Figure 2 (also by Korkegi, Kubota, and Mickey (1)) shows that extremely high Reynolds numbers are indeed encountered in the critical altitude range below 260,000 feet. It is only in this high Reynolds number regime that vehicle attitude may be effectively controlled or altered by aerodynamic means. Furthermore, the maximum aerodynamic loads and heating occur in this regime. Such high Reynolds numbers also produce turbulent boundary layer flow over most of the vehicle below 120,000 feet. Many flight characteristics differ markedly between laminar and turbulent flight regimes, especially the very critical heat transfer rate. These factors make it necessary, therefore, to obtain high Reynolds numbers in ground test facilities if adequate simulation of high velocity flight is to be obtained. It is for this reason that a great deal of interest is presently concentrated in developing high Mach number, high Reynolds number ground test facilities. Because the Reynolds number contains a geometric characteristic of the body being considered (usually the length), Figure 2 represents the trajectories of Figure 1 based on a body length of ten feet.

1. REGIMES OF HIGH VELOCITY FLIGHT

The fluid dynamic and chemical kinetic regimes of high velocity flight are shown in Figure 3, based on calculations of Probstein (2) and Harney (3), using a spherical vehicle of one-foot radius. The three basic flow regimes; continuum, transitional, and non-continuum, are characterized by the Knudsen number, which is the ratio of the molecular free path, λ, to a characteristic body dimension, ℓ, and is proportional

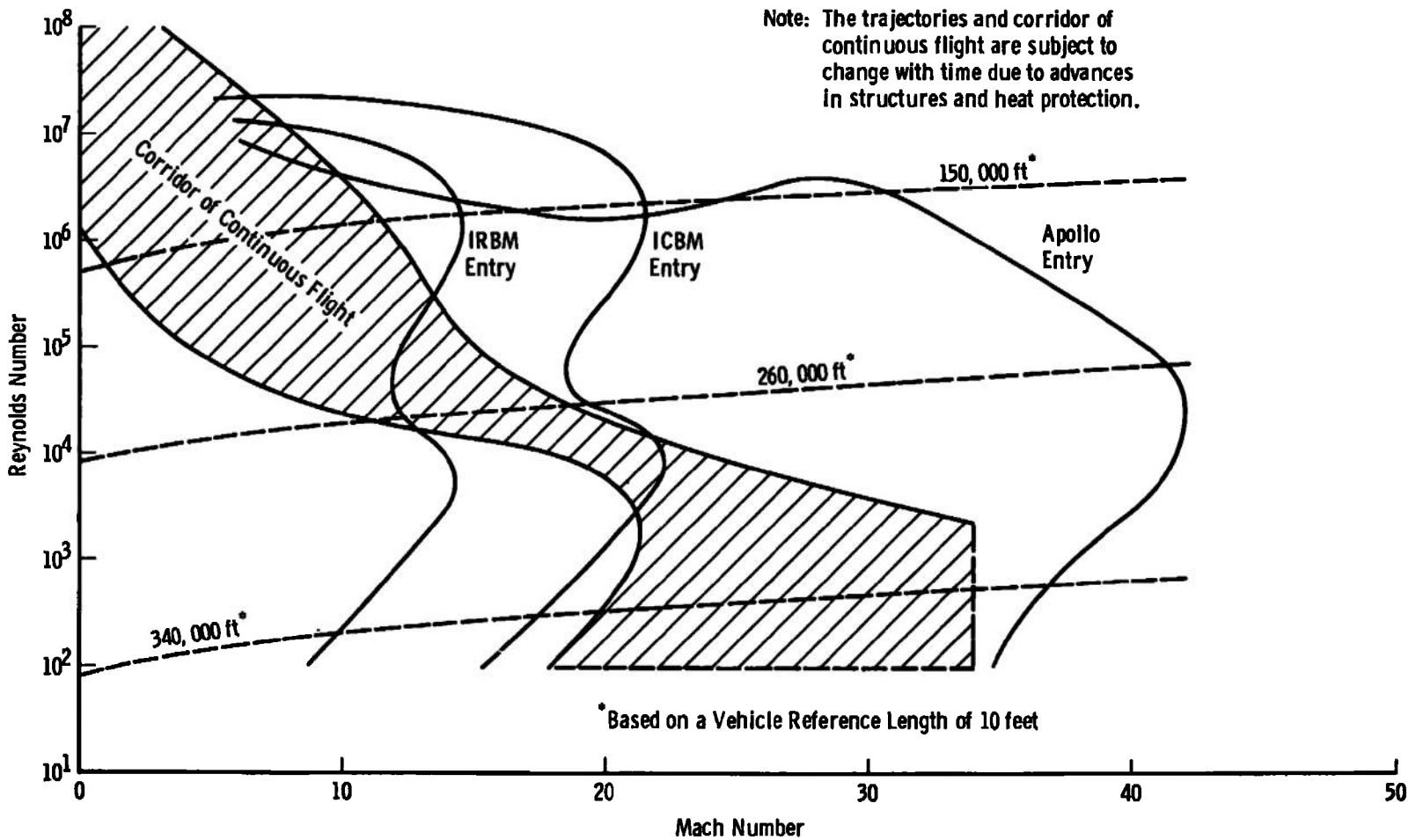

Figure 2. High Mach number, high Reynolds number flight regimes.

AEDC-TR-69-268

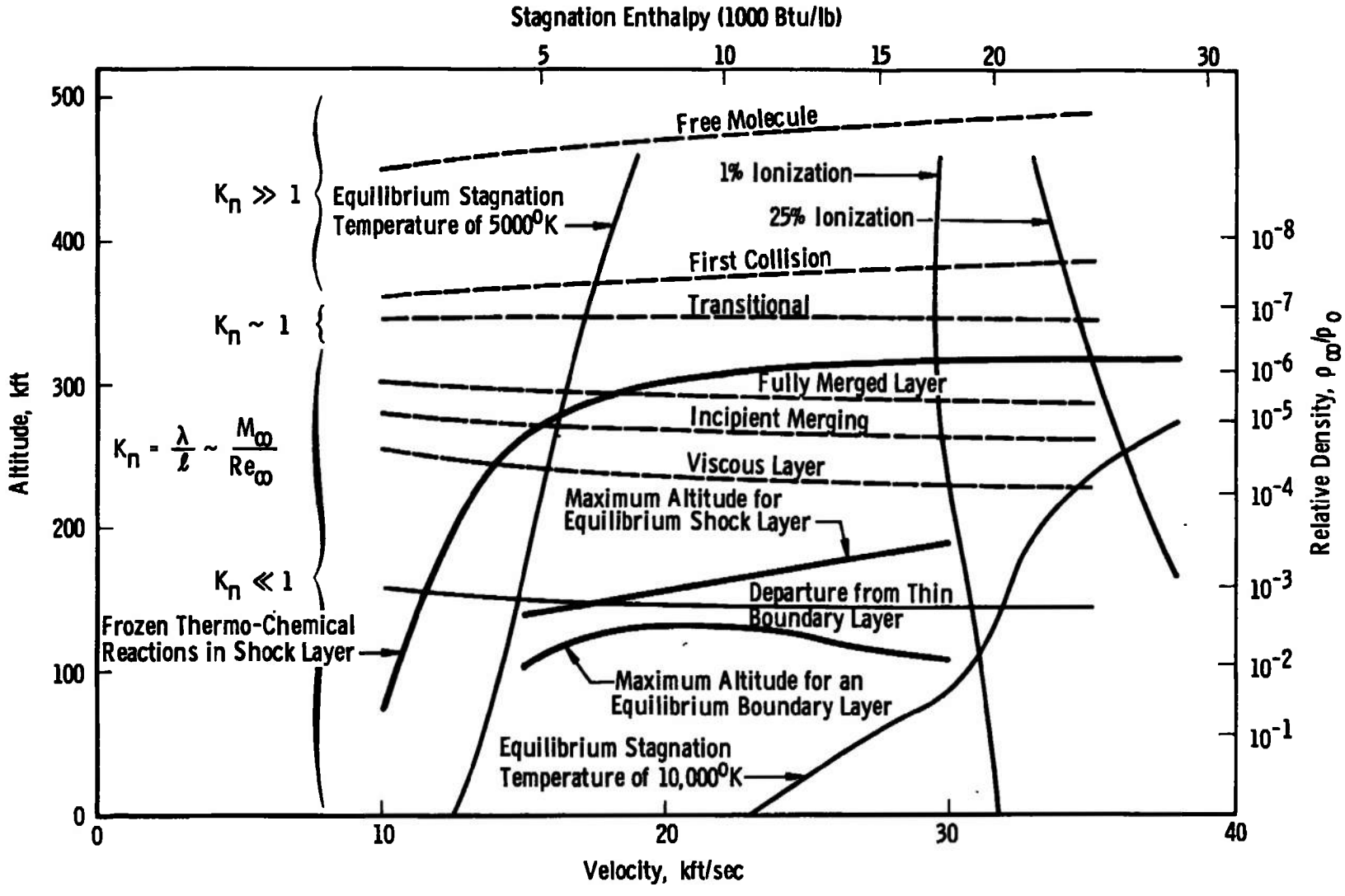

Figure 3. Hypersonic flow regimes.

to the Mach number over Reynolds number, thus:

$$Kn = \frac{\lambda}{\ell} \sim \frac{M_\infty}{Re_\infty} \qquad (1)$$

Continuum flow is characterized as Kn << 1, transitional as Kn ≈ 1, and free molecular or non-continuum as Kn >> 1. In the free molecular regime the ambient density is so low that molecules re-emitted from the vehicle surface after striking it, have no effect on incident molecules. At Mach 20 the mean free path must be of the order of 50 times the nose radius in order for the flow to be free molecular. As a vehicle further re-enters, it enters a regime described by the 'first order collision' theory. Here the Knudsen number is large, but not sufficiently large to insure the validity of the free molecular flow concept. This first order collision concept assumes that each incoming molecule has one collision with a re-emitted molecule before it reaches the vehicle surface. Re-entry flow conditions progress from the first order collision regime to a transitional regime marking the boundary between continuum and non-continuum flow. The Knudsen number here is order one, implying that the Mach number and the Reynolds number are of the same order of magnitude. For the one foot radius hemisphere of Figure 3, the continuum flow regime is reached at an altitude of approximately 340,000 feet. When continuum flow exists, certain mean quantities may be defined such as pressure, temperature, density, etc. and flow field characteristics such as boundary layers and shock waves defined. In the high altitude continuum regime, the Reynolds number is low and flow over the body is

dominated by viscous effects. Here both the boundary layer and shock wave are thick, and actually merge at lower densities as indicated in Figure 3, page 6. The high Mach number regime of present interest is seen to fall well within the area of continuum aerodynamics.

The regimes of thermo-chemical-kinetic effects due to high stagnation temperatures on high velocity flight vehicles are also shown in Figure 3. At high temperatures, the energy in non-ideal diatomic gases such as air goes into the vibrational energy mode in addition to the translational and rotational modes. Also energy can go into dissociation and ionization of the gas. Such a transfer of energy to these modes is referred to as 'real gas effects' or thermo-chemical-kinetic effects. As the high temperature stagnation region gas is expanded around the body, its temperature and pressure continuously decrease. The difference between the rate at which the conditions of the gas change, and the rate at which energy is liberated from the additional modes mentioned above determines whether the gas will be in an equilibrium state, a non-equilibrium state, or a 'frozen' flow state. In the equilibrium state, the reaction rates are high enough (i.e. the density and/or temperature great enough) that energy in the additional energy modes adjusts to the new flow conditions at a rate equal to the rate at which gas conditions are changing. Here the state of the gas is defined by the base composition and two thermodynamic properties. In the case of non-equilibrium, the reaction rates are lower than the rate at which gas conditions are changing, and not all of the energy is released from the additional energy modes. Hence for non-equilibrium, the state of the gas is a function of the gas properties, reaction rates,

time histories, and the rate of expansion. The rate of expansion is in turn a function of the body shape and size. In the frozen flow state the reaction rates are so low that virtually no adjustment can be made to the rapidly changing gas conditions. The energy in the additional energy modes is hence trapped or 'frozen' in these modes and the gas composition remains constant. Comparing Figures 1, 2, and 3, pages 2, 5, and 6, it is evident that real gas effects are significant in the regime of high Mach number, high Reynolds number flight and must be considered when wind tunnel simulation is discussed.

2. MACH NUMBER INDEPENDENCE

Relatively high Reynolds numbers can be obtained in continuous wind tunnels at low Mach numbers, but it becomes increasingly more difficult to obtain high Reynolds numbers as Mach number is increased, as shown in Section III. This problem is sometimes circumvented by considering a configuration to be Mach number independent above a certain limiting Mach number. For the flow to approach its limiting value, it is required that $M_\infty^2 \sin^2 \beta >> 1$ (where β is the shock angle). The value of the free stream Mach number for which the flow field becomes effectively independent of the Mach number will therefore depend on the geometry of the body, as well as on the value of γ. Thus the flow near the stagnation region of a blunt body with a detached shock will experience Mach number independence at a lower Mach number than the flow at some distance from the nose. Also, flow with an attached shock past relatively blunt cones will experience Mach number independence at lower Mach numbers than the flow past a

slender cone. The quantities which reach limiting values are those which determine the geometry of the flow behind the shock, i.e. the streamline inclination, the Mach angles, and the streamtube areas. The pressure coefficient also reaches a limiting value, but the ratios of pressure and temperature to the free stream values do not. These ratios increase as the square of the free stream Mach number for large values of the Mach number. The entropy jump across the shock also increases without reaching a limiting value.

An ever increasing body of experimental data (4,5) is demonstrating that the Mach number independence principle must be applied with care. One cannot say, a priori, that a given configuration will definitely exhibit Mach number independence. For example, Griffith and Boylan (4) have shown that even relatively blunt configurations such as Apollo have a dependence on Mach number far beyond the expected limit. Their data on the Apollo command module showed significant Mach number effects on static stability up to Mach 14. Cassanto, Rasmussen, and Coats (5) have presented a large body of data indicating a strong influence of Mach number on the laminar base pressure level and the radial distribution of base pressure. These data, taken over a Mach number range from 4 to 19, actually show Mach number dependence of the radial base pressure distribution becoming greater as high Mach numbers are approached. Stability characteristics of high lift-to-drag ratio re-entry configurations typically show Mach number dependence to Mach numbers as high as twenty.

Hence, the Mach number independence principle does not eliminate the need for high Mach number wind tunnel testing. While the principle

has been verified for certain parameters on some blunt and slender bodies, the Mach number continues to play an important role for many problems (notably aerodynamic stability) concerned with blunt-nosed slender configurations. It is obvious that both high Mach numbers and high Reynolds numbers are therefore required for many wind tunnel test programs if adequate and realistic flight simulation is to be obtained. We shall somewhat arbitrarily define the 'high Mach number regime' as discussed herein as $M \geq 10$. This is approximately the Mach number at which it becomes advantageous in ground testing to go to 'short run times' test facilities such as Hotshot and shock tunnels.

In this section, the regimes of high velocity flight have been investigated and from this discussion, four primary conclusions may be drawn. First, modern aerospace systems require simulation in the high velocity (high Mach number) regime. At the altitudes of primary interest, a second consideration, that of high Reynolds number simulation becomes important. Thirdly, thermo-chemical-kinetic effects in the flow about high velocity flight vehicles must be considered when discussing wind tunnel simulation. The fourth conclusion is that the high Reynolds numbers required for adequate ground simulation cannot be produced in wind tunnels by testing at a lower Mach number than flight, except for certain relatively simple bodies for which the Mach number independence principle holds. The next section will discuss specific wind tunnel requirements and related problems for simulation of high velocity flight.

SECTION II
WIND TUNNEL REQUIREMENTS FOR SIMULATION AND RELATED PROBLEMS

Flight simulation in ground test facilities[1] may be generally separated into two main categories: (1) real gas simulation, and (2) perfect gas simulation[2].

1. REAL GAS SIMULATION

Real gas simulation necessitates an attempt to recreate the environment of actual flight in a test facility and principally requires that stagnation enthalpy be duplicated. In doing so, the experimentalist matches free stream temperature and velocity of flight. The duplication of stagnation enthalpy manifests itself in the practical problem of creating (in the classical wind tunnel situation) extremely high reservoir pressures and temperatures, since the flow velocity is proportional to the 1/2 power of the reservoir enthalpy in a wind tunnel. This may be seen by considering an isentropic expansion and writing the energy equation as:

$$U_\infty = \sqrt{2(H_o - h_\infty)} \tag{2}$$

---

[1] We are concerned herein with flow simulators (i.e., wind tunnels), and not ballistic ranges.

[2] A perfect gas will be defined herein as one which is both thermally perfect (i.e., $P = \rho RT$) and calorically perfect (i.e., $\gamma = C_p/C_v$ = a constant).

For hypersonic Mach numbers, the free stream enthalpy is usually negligible. Figure 4, by Lukasiewicz (6), indicates the extremes of temperature, pressure, and input energy required for real gas simulation in the high Mach number regime. The energy requirements alone for real gas simulation of an Apollo or ICBM re-entry trajectory are obviously quite formidable. Allowing that such high energy levels might be obtained, the experimentalist is still confronted in the conventional wind tunnel with stagnation temperatures greater than 10,000°K. Severe deterioration of tunnel components plus excessive test gas contamination presently accompanies such temperatures. One critical aspect of this high temperature problem is throat heating. The limits imposed by throat heating on conventional wind tunnels are shown in Figure 5 which is by Potter (7). Presently this problem alone limits reservoir temperatures to less than 5000°K. Hence, a velocity no greater than 13,000 feet per second can be duplicated. As pointed out by several authors (7, 8, 9, 10), today 'real gas simulation' at high Mach numbers is not feasible in conventional wind tunnels.

2. PERFECT GAS SIMULATION

Perfect gas simulation offers an alternative and essentially means that only Mach number, Reynolds number, and γ are duplicated. The constraints imposed by these conditions are much less severe, but nevertheless formidable when high Reynolds numbers are desired in conjunction with high Mach numbers. Essentially perfect gas facilities match the flight Mach number, that is, they match the ratio of U_∞ to a_∞, and not

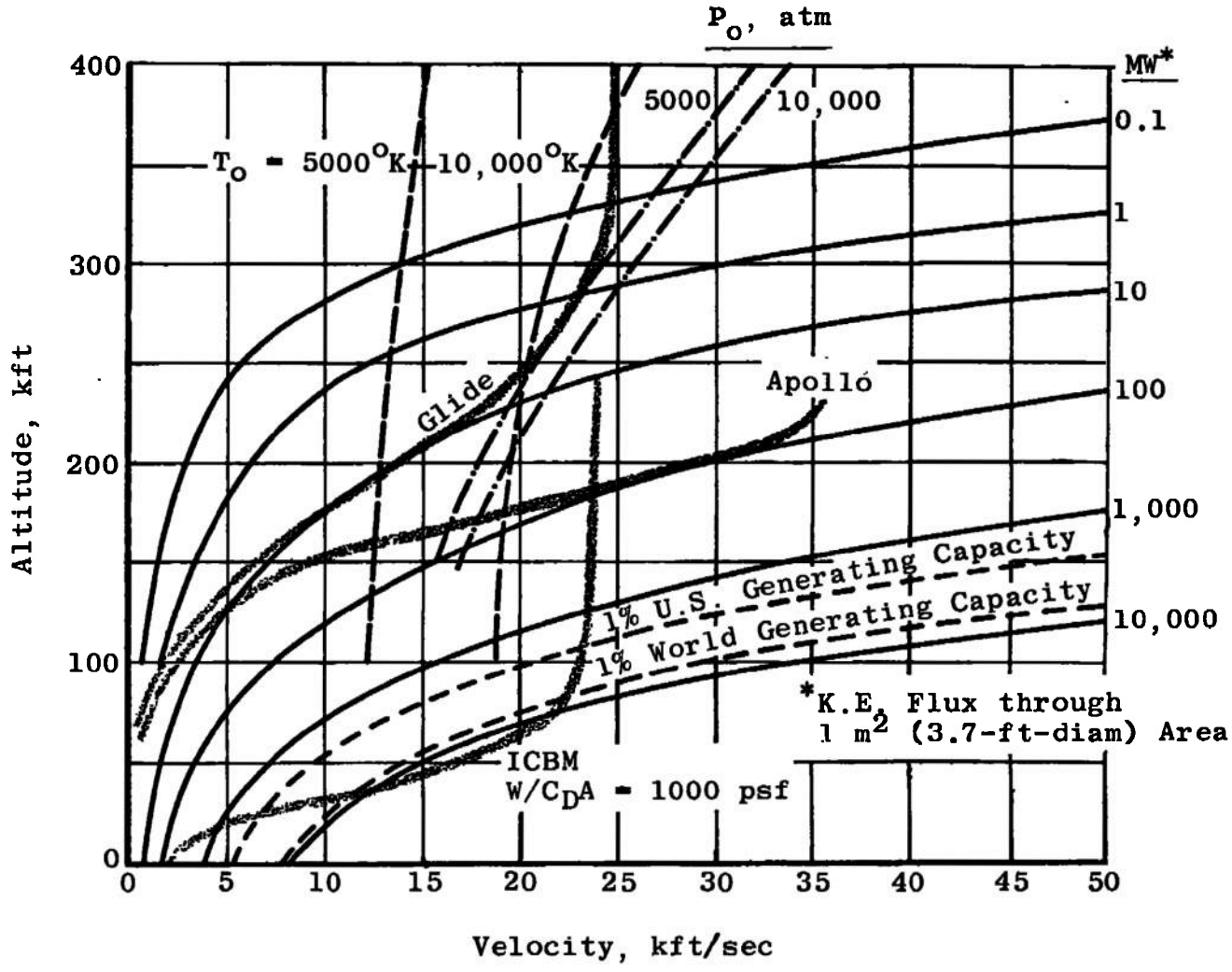

Figure 4. Requirements for real gas simulation.

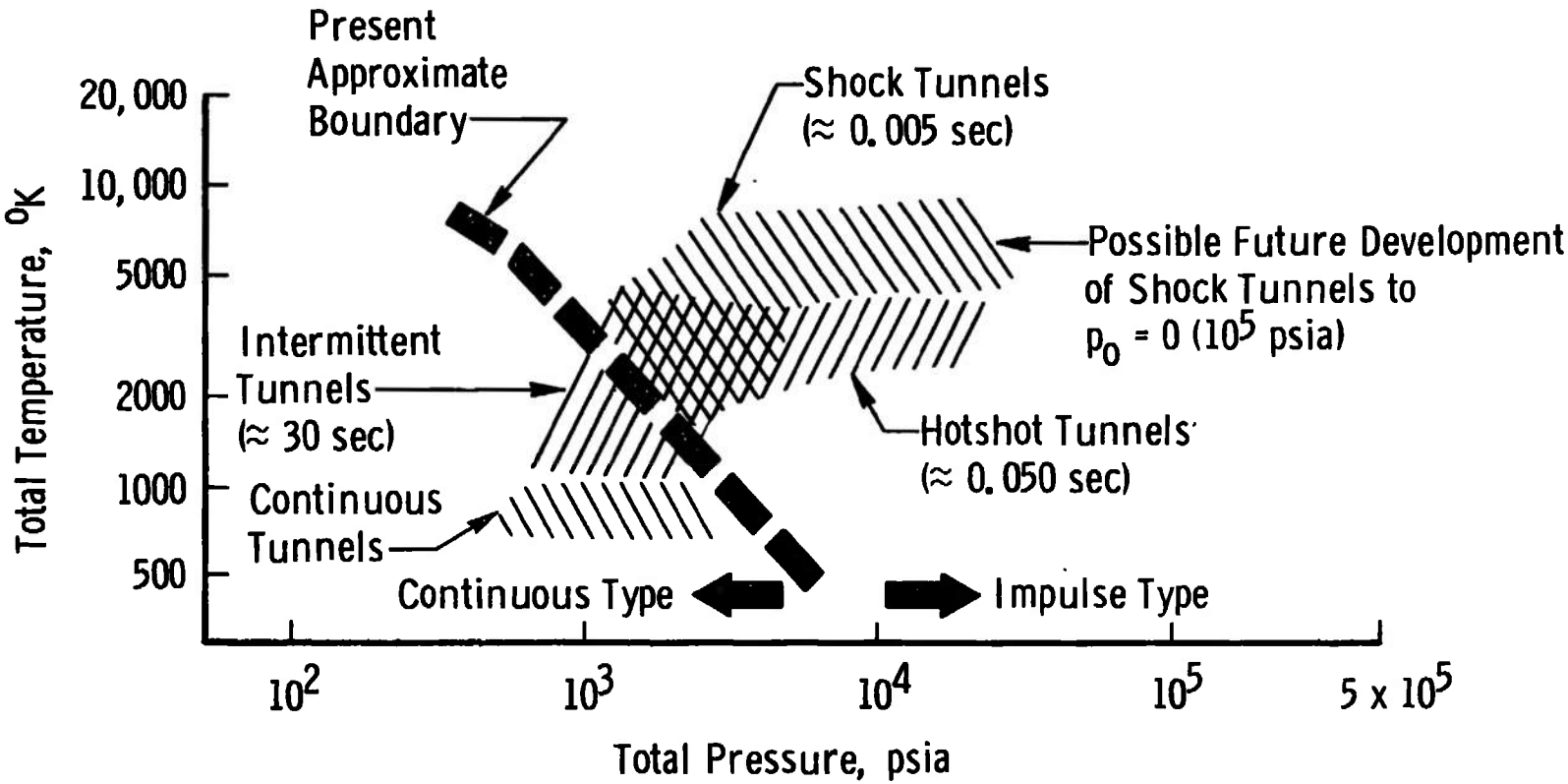

Figure 5. Approximate limits imposed on conventional wind tunnels by throat heating alone.

U_∞ and a_∞ separately as is done in real gas simulation. Also in perfect gas simulation, the free stream density is varied to match the flight and tunnel Reynolds numbers. Gas properties are matched by using a gas of the same specific heat ratio, γ. In the supersonic aerodynamic regime (M_∞ = 1 to 5), the perfect gas type simulation essentially duplicates flight conditions since real gas effects are negligible at low Mach numbers. However, for the hypersonic regime considered herein, the real gas effects discussed in Section I are not duplicated by perfect gas facilities. This is not, however, a serious compromise for many aerodynamic problems. Often the results of not duplicating these real gas effects can be predicted. The extreme conditions required for duplication of the stagnation enthalpy of flight are necessary primarily when nonequilibrium chemical processes must be completely simulated. In these cases, the time required for a given flow particle to move between any two points on the body must be the same in the wind tunnel test as in flight such that the ratio of flow time to reaction time is the same for both cases. When the chemical processes that occur are in equilibrium, or when they depend only on local conditions on the body, then scale models may be used. However, stagnation enthalpy must still be duplicated.

Since aerodynamic force is equal to the time rate of change of flow momentum between regions far upstream and downstream of the model, these forces are largely independent of real gas effects. Likewise most pressure measurements are not influenced by real gas effects and heat transfer measurements below Mach 25 (ionization occurs in flight

above Mach 25) can also be made which require easily introduced corrections. Notable exceptions to the last statement are base pressure measurements on flared bodies which are sensitive to the expansion at the base of the model, which in turn is a function of the ratio of specific heats on the flare, hence base pressure levels are greatly effected.

Chemical processes in hypersonic flight often take place only in a very localized region of the body such as nose and flared sections where high static temperatures exist. In such cases the effects of flow chemistry are generally small and can be investigated separately or corrections can easily be applied.

Figure 6 indicates the substantial benefits obtained in perfect gas simulation by allowing the expansion to proceed to the saturation limit of the test gas. This saturation limit is discussed in detail in Section III. This is in contrast to requiring 'real gas simulation' where $200°K \leq T_\infty \leq 300°K$. At Mach 14, for instance, the reservoir temperature may be reduced by a factor of three and one-half. At the reservoir pressure of 40,000 psi considered in this example, the reduction in total temperature is manifested in an increase in Reynolds number by a factor of 50. The limits imposed upon perfect gas simulation are essentially the same imposed upon real gas simulation, they simply occur at higher Mach and Reynolds number in perfect gas simulation. For instance, note in Figure 6 that a temperature as high as 2500°K is required to prevent condensation at Mach numbers around 18.

It will be shown in Section III that for perfect gas simulation

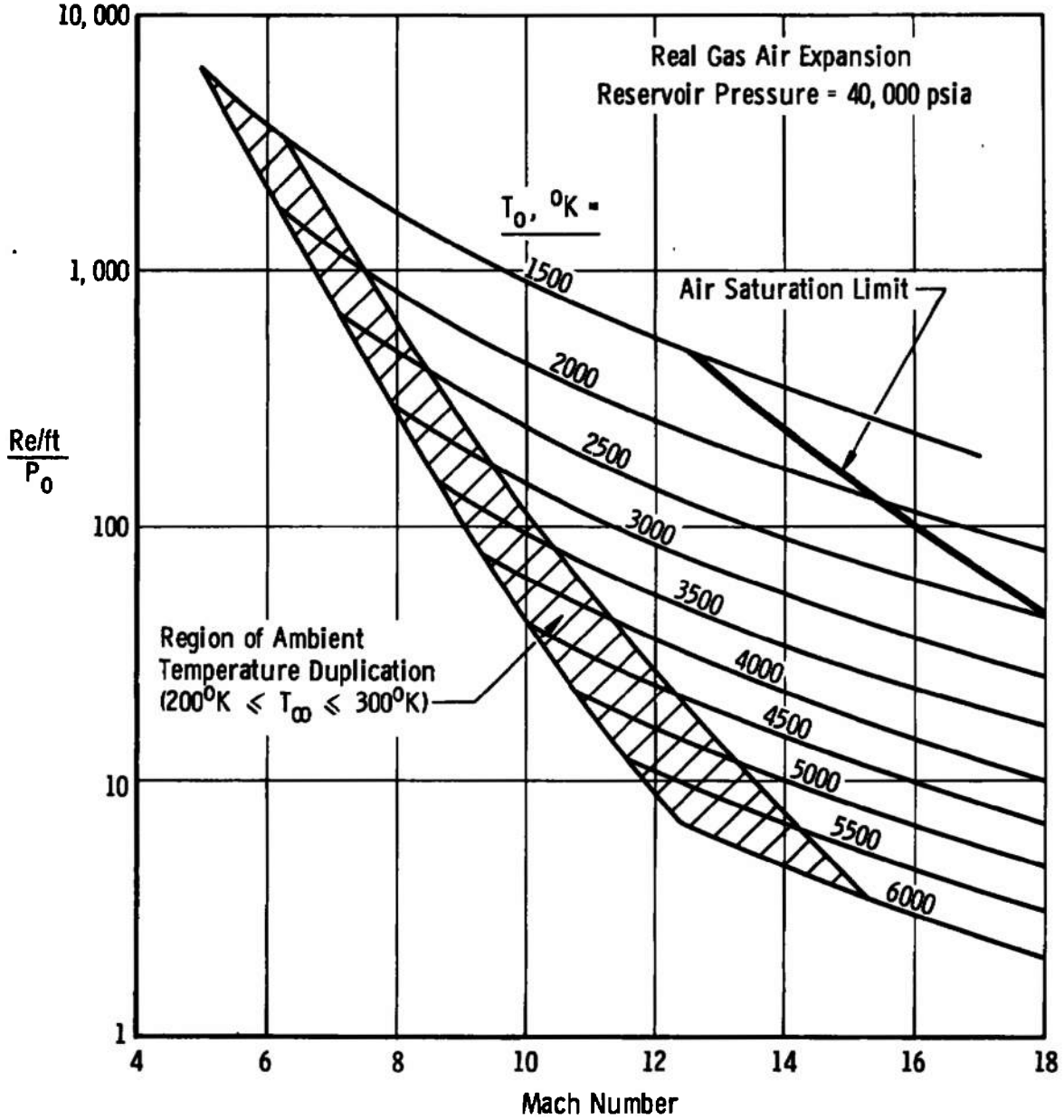

Figure 6. Reynolds number per foot vs. Mach number.

$$Re/ft \approx \frac{P_o}{\mu_\infty \sqrt{T_\infty}} f(M_\infty) \qquad (3)$$

Hence, for a given Mach number, with the reservoir temperature set by condensation limits (hence T_∞ and μ_∞ specified), the Reynolds number obtainable is directly proportional to the reservoir pressure. Increasing the reservoir pressures requires increased energy input. So although the stagnation enthalpy for perfect gas simulation is a factor of four below that for real gas simulation, the same fundamental constraints of high temperature, high pressure, and high energy input confront the experimentalist using perfect gas simulation.

Because of the numerous constraints mentioned above, a great deal of interest exists today in the development of perfect gas simulation. Therefore, a method will be developed in Section III to make predictions of perfect gas wind tunnel performance.

3. NON-EQUILIBRIUM IN WIND TUNNELS

Aside from the mechanical constraints mentioned above, chemical kinetic non-equilibrium in the test gas is often a limiting factor in both real and perfect gas wind tunnels. This should not be confused with the non-equilibrium flow about flight vehicles described in the preceding chapter. Here the chemical kinetic mechanism is the same, that is, some or all of the energy in the additional energy modes is trapped in those modes due to the rapid expansion, however in this case the non-equilibrium is in the free stream flow of the wind tunnel. The conventional wind tunnel expansion process requires high energy additions to the reservoir

gas to obtain high Mach numbers. The resulting high reservoir temperatures allow energy to go into the vibrational, and dissociational energy modes when non-ideal diatomic gases such as air or nitrogen are used. The approximate temperatures at which these energy modes are excited are given in Table I below. When the rate at which the temperature and

TABLE I
APPROXIMATE TEMPERATURES OF EXCITATION OF VIBRATIONAL, DISSOCIATIONAL AND IONIZATION ENERGY MODES IN AIR AND NITROGEN (P = 1 → 10 ATM)

Gas	Vibrational	Dissociational	Ionization
Nitrogen	1600°K → 2000°K	4500°K → 10,000°K	≥ 10,000°K
Air	1000°K → 1400°K	2500°K → 5500°K	≥ 10,000°K

pressure of the expanding test gas is decreasing (as it expands down the nozzle) is slower than the rate at which chemical reactions can occur in the gas, the energy in the additional modes is released and the free stream gas is said to be in equilibrium. However, when the expansion rate of the wind tunnel nozzle is of the same order as the reaction rate of the gas, non-equilibrium effects become important. In practice, wind tunnel nozzles cannot be made long enough to lower the expansion rate sufficiently to completely eliminate non-equilibrium under all high temperature conditions. Aside from physical constraints, such long nozzles would fill with thick boundary layers at hypersonic Mach numbers. The amount of non-equilibrium experienced in a given wind tunnel is a function of the particular geometry of that facility, being more severe as the rate of

expansion increases. For any given Mach number in any given wind tunnel, non-equilibrium effects are minimized by decreasing the reservoir temperature or increasing the reservoir pressure (as is the case for high Reynolds number testing). As with non-equilibrium flow about a flight vehicle, the term 'frozen' has been applied to the case of wind tunnel flow conditions in which the energy in the additional energy modes remains locked in these modes throughout the rapid expansion of the test gas. A model placed at the nozzle exit would then be exposed not to a hypervelocity stream of air, but rather to a flow consisting of a mixture of atoms and molecules. These non-equilibrium effects are usually measured in relation to their effect on the ratio of specific heats, γ, where $\gamma = 1.4$ for a perfect diatomic gas such as air or nitrogen.

Since perfect gas test facilities in high Reynolds number operation require extremely high reservoir pressures at relatively low reservoir temperatures, it is evident from the above discussion that non-equilibrium is usually not a problem. For real gas simulation, however, it most likely would be the controlling factor in performance.

4. SOURCE FLOW CONSIDERATIONS

Many advanced wind tunnel facilities presently use conical nozzles to expand the test gas. These nozzles offer several advantages over contoured nozzles, such as low design and procurement costs, relative ease of fabrication, and the capability of operating over a wide range of Mach number simply by changing throat sizes. The major

problem with these nozzles, however, is source flow effects and axial gradients in flow conditions. The expansion angle of the nozzle can be kept small, but practical limits of the cost of long nozzles plus the problem of boundary layer building on the nozzle walls limits practical nozzle half angles to four degrees or greater.

A conical model tested in source flow will experience an erroneous surface pressure proportional to the nozzle half angle, the cone angle, and the distance off centerline of a particular point on the body as pointed out by Whitfield and Norfleet (11). Using the nomenclature of Figure 7, a Newtonian analysis of the pressure at a point on the model yields:

$$P_E = 2\,\theta_c^{\,2}\,q_\infty \left(1 - 4\,\frac{\theta_N}{\theta_c}\,\frac{r_m}{r_N}\right) \qquad (4)$$

It becomes evident from this expression that the effect of source flow is a decrease in the level of surface pressure which would be experienced under parallel flow conditions. Furthermore, this decrease in pressure is large as the nozzle half angle (θ_N) and the distance off centerline (r) increase. Obviously, the nozzle half angle must be kept small and models kept to reasonable sizes to prevent significant errors. An error in total drag coefficient of -10 per cent results when testing a 9-degree half angle cone in a 100-inch diameter test section with a 4-degree half angle nozzle.

Non-equilibrium effects, discussed in the previous section, are also extremely sensitive to the nozzle half angle. If operation at

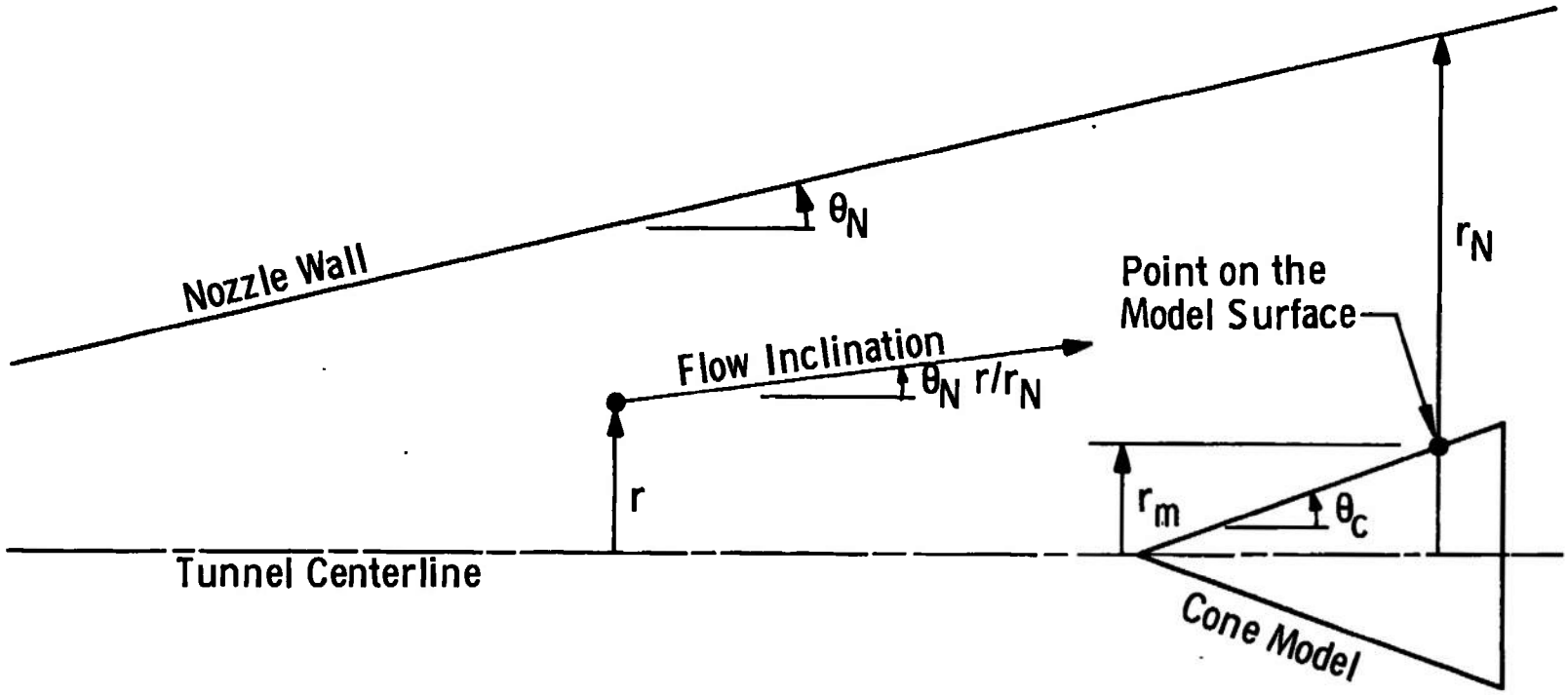

Figure 7. Nomenclature for the source flow analysis.

high temperatures and low pressures is conducted in perfect gas wind tunnels, the nozzle half angle must be kept small in order to keep non-equilibrium effects within reasonable limits.

5. RUN TIME CONSIDERATIONS

It has been previously stated that high Mach number simulation generally requires intermittent or short run time test facilities. This requirement primarily stems from throat heating considerations, high pressure requirements, and high energy input requirements resulting in energy storage devices. Perfect gas wind tunnels which operate continuously are usually limited to reservoir pressure around 2000 psia and reservoir temperatures below 1300°K (see Fig. 5). Intermittent wind tunnels, however, can presently be operated at reservoir pressures up to 50,000 psia and reservoir temperatures of 2500°K. Alternately, intermittent facilities can be operated at lower pressures and reach temperatures of up to 5000°K.

Short running times require fast response instrumentation. As the response of instrumentation becomes greater, the accuracy decreases. This problem is combined with the difficult requirement of measuring transient test conditions in short test time facilities. In continuous wind tunnels a pressure level of 0.1 psia or greater can be measured within ± 1 per cent. In "Hotshot" wind tunnels where test times range from 50 to 200 milliseconds, the same pressure range could be measured with ± 5 per cent accuracy. In shock tunnels where test times decrease to the order of 3 to 10 milliseconds the accuracy is ± 15 per cent.

While flow fields about a body usually are established within a millisecond, some phenomena such as supersonic combustion are studied with greater ease when test times are on the order of 100 milliseconds. Test times on the order of 100 milliseconds also allow the angle of attack of models to be varied during a run and permit models to be free flown in the wind tunnel.

Hence, it is generally advantageous to have long run times both from the standpoint of accuracy of measurements, from considerations of tunnel utility, and from the variety of testing techniques which may be employed.

SECTION III
CONSIDERATIONS FOR COMPARING PERFECT GAS WIND TUNNELS

As pointed out by Whitfield and Potter (9), there exists no single method of defining the basic criteria for simulation. Stokes' 1856 analysis of pendulum motion in viscous fluids revealed the relationship of fluid and geometric properties which yielded the basic aerodynamic simulation parameter called Reynolds number. This section will discuss the Reynolds number and other scaling parameters and determine a method for predicting performance and comparing perfect gas wind tunnels.

1. THE PRINCIPAL SCALING PARAMETERS OF PERFECT GAS SIMULATION

It can be shown that the equations of a continuum flow field (the Navier-Stokes equations, the continuity equation, and the energy equation) reduce to dimensionless forms involving certain scaling parameters. Under dimensional analysis with a thermodynamically ideal, steady, viscous, compressible flow assumed, these equations yield four principal scaling parameters:

Mach number $$M_\infty = \frac{U_\infty}{a_\infty} \tag{5}$$

Reynolds number $$Re_{\infty_\ell} = \frac{U_\infty \rho_\infty \ell}{\mu_\infty} \tag{6}$$

Prandtl number $$Pr = \frac{C_p \mu_\infty}{K_\infty} \tag{7}$$

Ratio of specific heats $\gamma = \frac{C_p}{C_v}$ (8)

In addition to the laws of motion, the boundary conditions lead to two additional secondary parameters:

Wall-to-free-stream temperature ratio T_w/T_∞

Geometrical length ratios (Shape)

In such an analysis the possibility of chemical activity in the gas is not considered. Motions with free surfaces, where gravitational forces must be considered, are also not included in this analysis. Such forces are included in similarity relationships by means of the dimensionless Froude number = $U/\sqrt{gd}$. As long as the gas is inert, the Prandtl number may be considered a secondary parameter also. The wall-to-free-stream temperature ratio is associated with the stimulation of the correct boundary layer characteristics and is important in hypersonic interaction problems.

The foregoing analysis indicates, as pointed out by Charwat (10):

> . . . that the Mach and Reynolds numbers can be meaningfully used as the principal coordinates for mapping out the characteristics of facilities in relation to fluid-dynamic problems. These parameters can be interpreted qualitatively as geometric 'scales' for the disturbed flow field relative to the model, which clarifies further their fundamental nature.

In this context, Charwat further points out that the Mach number may be thought of as a measure of the characteristic size of the model ($U_\infty t$) in relation to the extent of the field of convective disturbances ($a_\infty t$) such as pressure wave fields which are propagated at the speed of sound. In another context, the Mach number may be considered the ratio of the directed kinetic energy (U_∞^2) to the random thermal energy, $a_\infty = \sqrt{\gamma RT_\infty}$).

Likewise, the Reynolds number is a measure of the ratio of the model size to the size of a diffusional disturbance of the flow field (such as viscous boundary layers). Also it is commonly considered the ratio of fluid inertial force to viscous forces. Therefore, it is seen that the Mach and Reynolds numbers portray a 'distortion' of the flow field about the body. Charwat (10) points out that this concept is somewhat over-simplified since in supersonic and hypersonic flow the two processes are coupled and the convective and diffusional disturbance fields are embedded in each other.

As previously stated, perfect gas simulation implies the following criteria:

1. Matching the flight Mach number, that is, matching the ratio of U_∞/a_∞, rather than the quantities themselves.
2. Matching the gas properties by using a gas of the same γ.
3. Matching the flight Reynolds number.

Let us now examine the Reynolds number based on model length under perfect gas considerations:

$$Re_{\infty \ell} = \frac{\rho_\infty U_\infty \ell}{\mu_\infty} \tag{9}$$

Considering $P_\infty = \rho_\infty RT$ and $U_\infty = M_\infty \sqrt{\gamma\, RT_\infty}$

$$Re_{\infty \ell} = \left(\frac{P_\infty}{RT_\infty}\right) \ell \; \frac{M_\infty \sqrt{\gamma\, RT_\infty}}{\mu_\infty} \tag{10}$$

and expressing P_∞ in terms of M_∞ and P_o (perfect gas expansion assumed):

$$Re_{\infty_\ell} = \sqrt{\frac{\gamma}{R}}\,(\ell)\;\frac{P_o\, M_\infty \left[1 + \frac{\gamma-1}{2} M_\infty^2\right]^{\frac{-\gamma}{\gamma-1}}}{\mu_\infty \sqrt{T_\infty}} \tag{11}$$

Hence:

$$Re_{\infty_\ell} \sim \frac{P_o\, \ell}{\mu_\infty \sqrt{T_\infty}}\; f(M_\infty) \tag{12}$$

For a given Mach number, the Reynolds number is maximized by having the highest possible reservoir pressure, the largest possible model, and the lowest possible free stream temperature. The viscosity is, of course, a function of T_∞. The four parameters P_o, ℓ, T_∞, and μ_∞ will now be examined in order to indicate how Reynolds number may be maximized and under what consideration wind tunnel performance may be compared.

2. RESERVOIR PRESSURE

Reservoir pressure and tunnel size are the principle variables in determining the maximum Reynolds number performance of a wind tunnel. The temperature, T_∞, and viscosity μ_∞ are specified by condensation limits which will be discussed later. Given a tunnel sized by economic considerations, the experimentalist must then seek to obtain the highest possible P_o. As pointed out previously, for high Mach number operation, high reservoir pressure can only be achieved by using intermittent facilities with short run times.

Considering a fixed volume reservoir V, the increase in reservoir pressure ΔP is proportional to the added energy ΔE, or:

$$\Delta P \sim \frac{\Delta E}{V} \tag{13}$$

Pressures of 40,000 to 50,000 psia can presently be accommodated in short duration wind tunnel reservoirs. Assuming that an adequate pressure vessel can be developed for such high pressures, the wind tunnel designer must then develop a reasonable energy-volume relationship. The reservoir volume in fixed volume facilities is set such that reasonable decay rates of pressure are obtained. Hence, a large test section requires a large reservoir to prevent excessive decay and, in turn, requires large energy input. The energy input is, of course, a significant factor in cost of operation and for a given reservoir size and pressure is a function of the temperature required to prevent test gas saturation. The considerations of decay rate are generally qualitative and are functions of the type of testing to be done in the facility. However, the lower the decay rate in a wind tunnel, the greater the tunnel utility. Osgerby and Smithson (12) have shown that testing of scramjet propulsion units in a Hotshot wind tunnel (fixed volume reservoir) is strongly dependent on decay rates. They point out that that the adequacy of a wind tunnel for scramjet testing decreases rapidly as decay rates increase. Osgerby and Smithson found the AEDC-VKF Tunnel F (which is discussed in Section IV) to be well suited for combustion research since decay rates with a four cubic foot reservoir could be kept on the order of 0.1-per cent per millisecond.

3. WIND TUNNEL SIZE

The dimensional term, ℓ, in the Reynolds number equation (Equation 12, page 29) represents any characteristic body dimension such as model length. The largest possible model is required to maximize the Reynolds number and its size is related closely to the test section size. Therefore, the physically larger wind tunnel has an advantage over a smaller tunnel if the same unit Reynolds number is produced in both tunnels. The cost of building and operating wind tunnels increases rapidly as tunnel size is increased, hence economic factors rather than aerodynamic factors tend to control the length term in Equation 12.

In order to make a fair comparison between facilities we shall follow a general rule that the maximum model length is seldom longer than the test section useful diameter. This is the diameter of the region not affected by wall boundary layers and is commonly called the 'test section core' diameter. In cases where the test section core diameter is not known, it may be estimated by using the hypersonic wind tunnel turbulent boundary layer thickness correlation of Edenfield (13) which is:

$$\frac{\delta}{x} = 0.195 \frac{M_\infty^{0.375}}{Re_{\infty_x}^{0.166}} \tag{14}$$

Edenfield's equation has been shown to agree well with experimental data for $M_\infty \geq 10$. This treatment of the length variable in the Reynolds number equation correctly gives the physically larger test facilities an advantage in obtaining high Reynolds numbers.

4. TEMPERATURE CONSIDERATIONS

The lower limit on the free stream temperature is set by condensation and/or saturation of the test gas or water vapor. The problem of water vapor condensation is easily solved by drying the test gas. The condensation and saturation points of the test gas are known functions of pressure and temperature. Daum and Gyarmathy (14) have investigated these limits for both air and nitrogen in hypersonic wind tunnels. Some of these results are shown in Figure 8. Many test facilities are operated only a few degrees above the experimentally determined condensation point of the test gas, instead of at the theoretical saturation temperature. The gain in Reynolds number by using this procedure is obvious from equation 12, page 29, which indicates that the gain in Reynolds number is inversely proportional to the free stream temperature. This procedure is particularly attractive in test facilities using nitrogen as can be seen in Figure 8, since the experimental condensation point is 15 to 20 degrees below the theoretical saturation limit. There does not exist enough data such that the experimentalist can be assured, a priori, that supercooling of the test gas beyond the theoretical saturation limits will not invalidate the experiment. The degree of supercooling which may safely be allowed is a function of the nature of the model being tested and the type of data being obtained. In order to establish a uniform basis of comparison, therefore, it is necessary that the minimum allowable free stream temperature to be considered in performance estimates herein be defined as the theoretical saturation lines described in Figure 8.

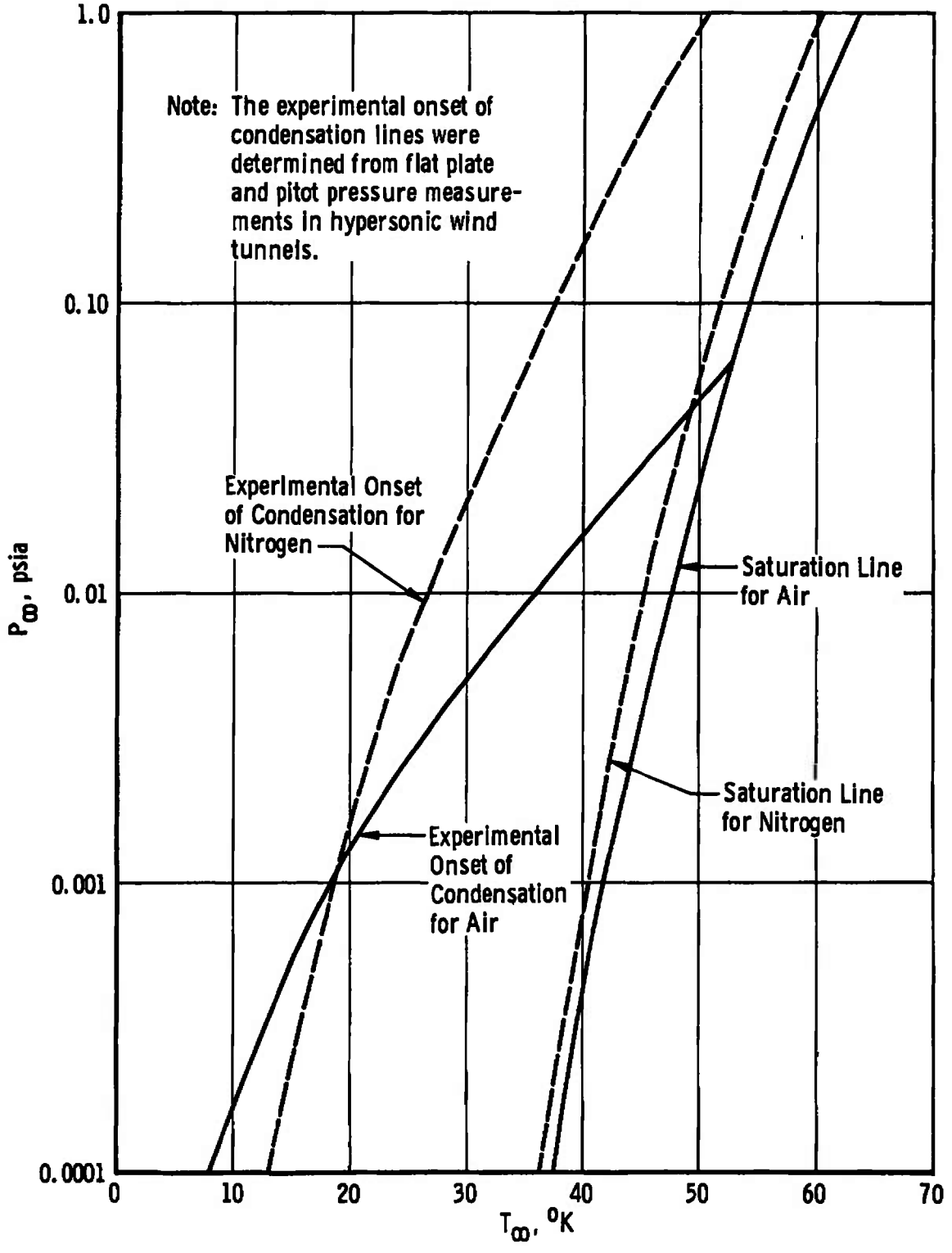

Figure 8. Condensation and saturation limits for air and nitrogen.

5. VISCOSITY

Equation 12, page 29, indicates that Reynolds number is inversely proportional to viscosity. Today, many authors (15, 16, 17, 18) have presented viscosity relations which are often used indiscriminently by others without regard to their consistency or accuracy in a given temperature range. While all the common viscosity relations agree within ± 2 per cent for temperatures of $300 \leq T \leq 1000°K$ (at a pressure of one atmosphere) significant discrepancies appear outside this range. An extensive compilation of theoretical and experimental data at AEDC indicates that the classical Sutherland equation is accurate above 100°K but gives values less than those obtained experimentally below this temperature. As indicated by Figure 8, hypersonic wind tunnels operating at saturation temperature for perfect gas simulation have free stream temperatures around 40 to 60°K. Use of the Sutherland equation for calculations of perfect gas wind tunnel performance will, therefore, give an erroneously high value of Reynolds number. The experimental data which are based on Reynolds number correlations from hypersonic wind tunnels support the approach of Fiore (18), who suggests that a linear viscosity relation be used below 100°K. Hence, an accurate determination of viscosity should be based on a linear relation below 100°K and the Sutherland equation above 100°K. These relations are:

Linear

$$\mu_\infty = \frac{T_\infty}{10} \frac{K_1}{1 + \frac{K_2}{100}} \qquad T_\infty \leq 100°K \tag{15}$$

Sutherland $$\mu_\infty = \frac{K_1 \sqrt{T_\infty}}{1 + \frac{K_2}{T_\infty}} \qquad T_\infty \geq 100°K \tag{16}$$

where for air:

$$K_1 = 3.0485 \times 10^{-8} \qquad K_2 = 112°K$$

and for nitrogen:

$$K_1 = 2.9511 \times 10^{-8} \qquad K_2 = 112°K$$

At 40°K with nitrogen as a test gas, the difference between these two relations is 10 per cent. The combination of the linear and Sutherland viscosity formulas described above is used in all performance calculations in this report.

6. NITROGEN AS A TEST GAS

It is common practice in high Reynolds number perfect gas facilities to substitute nitrogen for air as the test gas. Aside from the obvious advantage of not having oxidation of tunnel components due to high temperature air, another important advantage may be noted from Table I, page 20. Both the vibrational and dissociational energy modes are excited at a higher temperature in nitrogen. Hence the non-equilibrium limits may be eliminated or at least significantly increased to higher values of reservoir temperature. The similarity conditions previously discussed are met when substituting pure nitrogen for air since both Prandtl number, Pr, and the ratio of specific heats, γ, are approximately reproduced.

7. REAL GAS EXPANSIONS

If the free stream conditions of a perfect gas wind tunnel are calculated using perfect gas relations to describe the entire expansion, significant error will result. This is so because the test gas is at a very high temperature during the initial part of the expansion process. These high temperatures produce changes in the ratio of specific heats, γ, to which the expansion process is extremely sensitive. This dependence on γ is clearly shown in Equation 11, page 29. When using perfect gas relations to describe the expansion a $\gamma = 1.4$ value is usually assumed throughout the expansion process. This difficulty is easily overcome by using tabulated thermodynamic data for constant values of entropy such as that of Neel and Lewis (19, 20). A Mollier diagram, which is a graphical representation of thermodynamic properties, may also be used when accuracy is not critical. When using tables, the value of the dimensionless entropy, S/R, is determined which corresponds to the given reservoir conditions. Throughout an isentropic expansion, the entropy is of course constant, and only that particular table is used which corresponds to this determined value of reservoir entropy. At the appropriate values of both reservoir and free stream temperature in this table, the corresponding values of density, pressure, or enthalpy can be read. The free stream velocity is then calculated by the energy equation in the form:

$$H_o = h_\infty + 1/2\, U_\infty^2 \tag{17}$$

or:

$$U_\infty = \sqrt{2(H_o - h_\infty)} \tag{18}$$

and the speed of sound can be determined by:

$$a_\infty = \sqrt{\gamma R T_\infty} \tag{19}$$

and of course Mach number is then determined by U_∞/a_∞. The Reynolds number is then calculated using Equation 6, page 26. These calculations are easily performed over a wide range of reservoir conditions by computer. Edenfield[1] has obtained previously unpublished computer solutions for Mach number and Reynolds number corresponding to various values of reservoir pressure and temperature using both real air and real nitrogen gas properties. These data are presented graphically in the Appendix. The saturation limits on these plots correspond to the saturation lines of Figure 8, page 33.

8. SUMMARY OF COMPARISON CRITERIA

The comparison of high Mach number, high Reynolds number perfect gas test facilities will be based on the following six criteria:

1. All estimates of performance should be based on quoted operating ranges of the reservoir temperature and pressure (or the equivalent enthalpy and entropy).
2. The real gas expansions of the Appendix will be used to determine unit Reynolds number over the quoted Mach number, reservoir pressure, and reservoir temperature range.

---

[1]Emmett E. Edenfield of the Aerodynamics Section, Hypervelocity Branch, von Karman Gas Dynamics Facility, Arnold Engineering Development Center.

3. The reservoir test gas is assumed to be expanded to the saturation temperature as given in Figure 8, page 33.
4. The viscosity used in the calculation of Reynolds number will be obtained by using a linear relation for viscosity below 100°K (Equation 15, page 34) and the Sutherland viscosity formula (Equation 16, page 35) above 100°K. The data of the Appendix are based on these viscosity relations.
5. The length term in the Reynolds number equation (Equation 6, page 26) should be taken as the experimentally determined core diameter, or a calculated core diameter using Equation 14, page 31, and geometric dimensions.
6. Since high Reynolds number conditions are to be compared, non-equilibrium effects will be assumed negligible.

SECTION IV
SELECTED COMPARISONS OF TEST FACILITIES

As an example of how the criteria outlined in Section III are applied, a comparison will now be made of four high Mach number, high Reynolds number test facilities which reflect the state of the art for each type of facility. These facilities will be compared on the Mach-Reynolds number basis using an identical scale in all figures so as to preserve a proper perspective. Only by applying a common set of criteria, can test facility performance be accurately compared in this manner. Most technical reports describing the performance of a particular perfect gas wind tunnel present data on a Mach number-Reynolds number basis. These reports do not generally indicate, however, what criteria were used for defining viscosity and temperature limits. Quoted reservoir operating conditions are not subject to such arbitrary definitions, hence, they can safely be used as indicated below to compare test facilities. In these comparisons, both Reynolds number based on wind tunnel core diameter, Re_{∞_D}, and Reynolds number per foot, Re/ft, are presented in order to illustrate the benefits of a physically large wind tunnel.

1. THE AEDC-VKF TUNNEL "F"

Tunnel "F" is located in the von Karman Gas Dynamics Facility (VKF) of the Arnold Engineering Development Center (AEDC), Tullahoma, Tennessee. It is of the "Hotshot" type tunnel which utilizes

an electric arc discharge to heat air or nitrogen to high reservoir temperatures and pressures. The test gas is initially confined in a one to four cubic foot "arc chamber" by a diaphragm located near the throat of its conical nozzle. The nozzle, test section, and dumptank are at the same time evacuated to low pressure. Upon arc discharge, which lasts about 20 milliseconds, the test gas is heated to high pressure and temperature and the diaphragm ruptures. The test gas is subsequently expanded to either of two test sections. A 54-inch diameter test section located half way down the conical nozzle covers a Mach number range from 10 to 19, while a 108-inch test section located 64 feet down the nozzle covers a Mach number range of 13 to 23. The nozzle half angle is four degrees in order to minimize non-equilibrium effects and source flow effects. Test times vary from 100 to 200 milliseconds. The maximum arc chamber conditions for high Reynolds number operation using nitrogen as a test gas are P_o = 40,000 psia and T_o = 2700°K. Under these conditions the maximum size throat diameter (2 inches) yields M_∞ = 11 in the 54-inch test section and M_∞ = 14 in the 108-inch diameter test section. The minimum throat diameter, 0.35-inch yields Mach 19 in the 54-inch test section and Mach 23.5 in the downstream 108-inch test section. Figure A-1e, page 69 of the Appendix shows immediately that the Mach 23.5 condition in the 108-inch test section cannot be attained under the maximum Reynolds number constraint of $T_{o_{max}} \leq 2700°K$. Mach 19 is the highest obtainable Mach number if $T_{o_{max}} \leq 2700°K$ and operation along the theoretical saturation line is specified. This Mach number is obtained in the 108-inch test section using a 0.75-inch diameter throat.

Higher Mach numbers of course can be attained at lower reservoir pressures where higher temperatures can be tolerated. For example, Tunnel F can be operated at 4000°K at 20,000 psia. Under such conditions Mach numbers as high as 24 are reached, however, the unit Reynolds number is only 0.12×10^6 as indicated in Figure A-1c, page 67, of the Appendix.

The use of a fixed volume arc chamber means that the reservoir pressure, P_o, will decay exponentially with time. Since data may be taken only after starting transients have settled out (approximately 40 milliseconds), the full 40,000 psia maximum pressure is unuseable for useful aerodynamic testing. Hence, for a 2-inch diameter throat using the empirical correlation for decay rates of Eaves, Griffith, and Buchanan:[1]

$$\frac{P_o}{P_{o_{max}}} = e^{-6.17 \times 10^{-6} \, T_o \frac{d^{*2}}{V} t} \qquad (20)$$

where t is in milliseconds, we therefore have:

$$(P_o)_{40 \text{ msec}} = 0.75 \, (P_{o_{max}}) = 30{,}000 \text{ psia.}$$

Now Figure A-1e, page 69, of the Appendix gives at Mach 11 and 30,000 psia in nitrogen:

$$\frac{Re/ft}{P_o} = 1000 \qquad \text{at } T_o = 1300°K$$

Therefore we have:

$$Re/ft = 30 \times 10^6 \qquad \text{at } M_\infty = 11$$

To determine the test section core diameter the boundary layer thickness will be calculated from Equation 14, page 31, using a length, x, of 32 feet from the throat to the test section. Hence:

[1]Hypervelocity Branch, von Karman Gas Dynamics Facility, Arnold Engineering Development Center.

$$\frac{\delta}{x} = 0.195 \frac{M_\infty^{0.375}}{Re_{\infty_x}^{0.166}}$$

$$= \frac{0.195\ (11)^{0.375}}{(32)(30 \times 10^6)^{0.166}}$$

$$= 0.154$$

Therefore, δ = 6.0 inches and the core diameter is 54- 2(6.0) = 42 inches, and the Reynolds number based on test section core diameter becomes

$$Re_{\infty D} = \frac{42}{12} (30 \times 10^6) = 105 \times 10^6$$

The other limiting points yield the results shown in Table II below.

TABLE II
MAXIMUM REYNOLDS NUMBER PERFORMANCE OF TUNNEL F

Test Section Diameter	d* in.	P_o psia	M_∞	$\frac{Re/ft^{(1)}}{P_o}$	$T_o^{(1)}$ °K	$\delta^{(2)}$ ft.	$Re_{\infty D}$
54-in.	2.00	30,000	11	1000	1300	0.50	105×10^6
54-in.	0.75	37,500	15	150	1850	0.73	17×10^6
54-in.	0.35	39,000	19	33	2700	1.04	3×10^6
108-in.	2.00	30,000	14	240	1700	1.22	47×10^6
108-in.	1.25	36,600	16	105	2100	1.43	24×10^6
108-in.	0.75	37,500	19	33	2700	1.82	6.5×10^6

(1) This value is obtained from Figure A-1e, page 69, of the Appendix.

(2) This value is obtained by using Equation 14, page 31.

These data are graphically illustrated in Figure 9. The upper limit defined by the maximum pressure is herein assumed to vary linearly between any two calculation points. The increments in Mach number at which calculations should be made to avoid significant errors varies from $\Delta M = 2$ around Mach 8 and 10, to $\Delta M = 4$ at Mach 12 to 16, and $\Delta M = 6$ at or above Mach 20.

The limits imposed by the maximum decay rate (for $d^* = 2.0$-in.) is not a vertical line on the Reynolds number-Mach number scale of Figure 9. This decrease in Mach number results from an increasing boundary layer displacement thickness as the Reynolds number is decreased. When comparing the maximum Reynolds number performance of a given facility, therefore, it is extremely important to know the Mach number range which corresponds to the maximum Reynolds number operating conditions, and not merely the total Mach number range. In the case of Tunnel F, the estimates for the lower Mach number limit at low Reynolds numbers (low P_o) is Mach 9.7. As previously stated, however, Mach 11 corresponds to the minimum Mach number attained at the maximum Reynolds number conditions of $P_{o_{max}}$ = 40,000 psia.

It should also be noted in Figure 9 that at a given Mach number both test sections of Tunnel F give similar performance on a Reynolds number per foot basis. The large size of the 108-inch diameter test section becomes a significant advantage, however, when comparing test sections on the Re_{∞_D} basis.

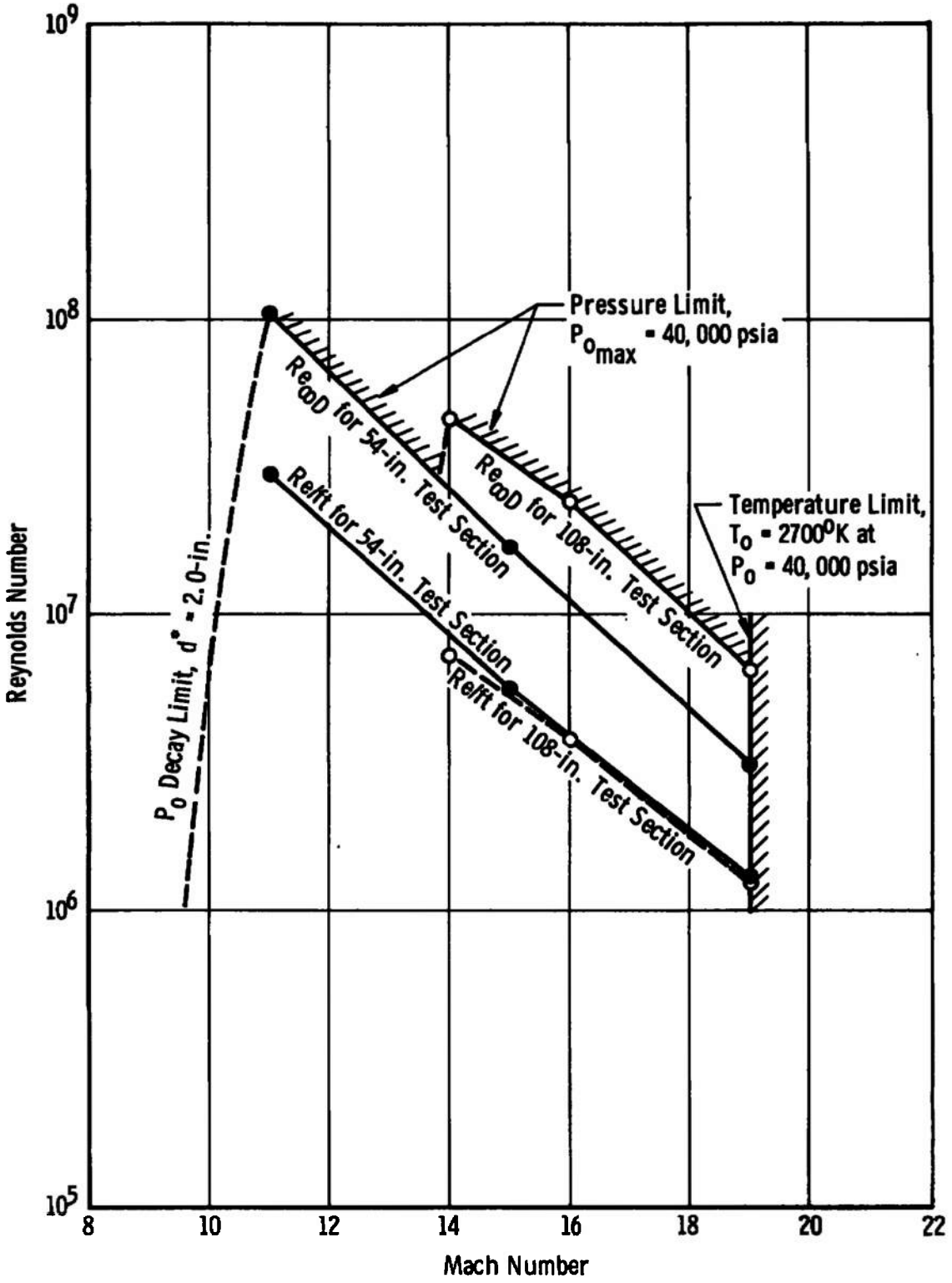

Figure 9. Maximum Reynolds number performance of the AEDC-VKF Tunnel F.

2. THE CORNELL AERONAUTICAL LABORATORY HYPERSONIC SHOCK TUNNEL (96-IN. LEG)

The Cornell Aeronautical Laboratory's Hypersonic Shock Tunnel (96-in. leg) is a high performance, driver heated shock tunnel (21). This type of test facility and its theory of operation are described in detail by many authors (9, 22, 23, 24). This tunnel consists of a 5-inch I.D. driver of 16 foot length, a 4-inch I.D. driven tube 48.5 feet long, a nozzle section in which one of four nozzles may be placed, and a 96-inch diameter combined test section and vacuum tank.

The operation of this facility, which is typical of high performance shock tunnels, consists first of charging the driver section to pressures as high as 30,000 psia. The temperature of this high pressure driver gas (which may be either helium or hydrogen), is raised to 700°K by means of an external resistance heater. The driven section, separated by a double diaphragm from the driver section, is pressurized with air or nitrogen (the test gas) such that the ratio of driver gas pressure to driven gas pressure is a certain value, typically on the order of 10,000. This pressure ratio, the temperature ratio, and the ratio of molecular weights of the driver gas to the driven gas determine the performance of the shock tunnel. A light diaphragm separates the driven tube from the nozzle and vacuum tank which are evacuated to low pressure by means of vacuum pumps. When the double diaphragm is ruptured, the driver gas preceded by a high strength shock wave, moves into the test gas in the driven tube, heating and compressing the test

gas. The diaphragm separating the driven tube and the nozzle is of sufficient strength that it will reflect the incident shock wave before rupturing and hence the shock wave further heats and compresses the test gas as it returns up the tube. The Cornell Hypersonic Shock tunnel is operated in the tailored interface mode. In this mode of operation the interface between the driver gas and the test gas is brought nearly to rest by the reflected shock wave. This creates a relatively constant reservoir pressure and temperature for short time (5 to 10 milliseconds) which is then expanded into the test section without pressure or temperature decay. Operating in this mode with a maximum driver pressure of 30,000 psia, this facility obtains reservoir conditions behind the reflected shock of P_o = 20,000 psia, and temperatures as high as 4000°K. The test gas is expanded by means of one of the four nozzles described in Table III. The Mach number ranges given in Table III are total Mach

TABLE III
NOZZLES FOR THE CORNELL HYPERSONIC SHOCK TUNNEL (96-IN. LEG)

Nozzle Exit Diameter	Type of Nozzle	Exit Mach Number
24-in.	Contoured	6.5 - 8.2
48-in.	Contoured	10.0 -17.0
48-in.	10.5° Half Angle Cone	7.0 -22.0
72-in.	10.5° Half Angle Cone	8.6-24.0

number ranges and do not correspond to the Mach number range at maximum Reynolds number conditions. Considering operation at or above Mach 8, the maximum Reynolds number performance parameters for the 24-inch contoured nozzle, the 48-inch conical nozzle, and the 72-inch conical nozzle are given in Table IV. These data are presented graphically in Figure 10.

TABLE IV
MAXIMUM REYNOLDS NUMBER PERFORMANCE OF THE CORNELL HYPERSONIC SHOCK TUNNEL (96-IN. LEG)

Nozzle	M_∞	$\frac{Re/ft^{(1)}}{P_o}$	Re/ft	$T_o^{(1)}$ °K	$\delta^{(2)}$ ft.	$Re_{\infty D}$
24-in.	8.0	6000	120.0×10^6	880	0.20	190.0×10^6
48-in.	8.5	3500	70.0×10^6	950	0.22	250.0×10^6
48-in.	10.0	1300	26.0×10^6	1150	0.28	90.0×10^6
48-in.	12.0	470	9.4×10^6	1500	0.35	31.0×10^6
48-in.	16.0	90	1.8×10^6	2100	0.50	5.4×10^6
48-in.	22.0	12	0.2×10^6	3350	0.81	0.6×10^6
72-in.	10.0	1300	26.0×10^6	1150	0.28	141.0×10^6
72-in.	12.0	470	9.4×10^6	1500	0.35	50.0×10^6
72-in.	16.0	90	1.8×10^6	2100	0.50	9.0×10^6
72-in.	24.0	6.6	0.1×10^6	3900	0.92	0.5×10^6

(1)This value is obtained from Figure A-1c, page 67, of the Appendix.

(2)This value is obtained by using Equation 14, page 31.

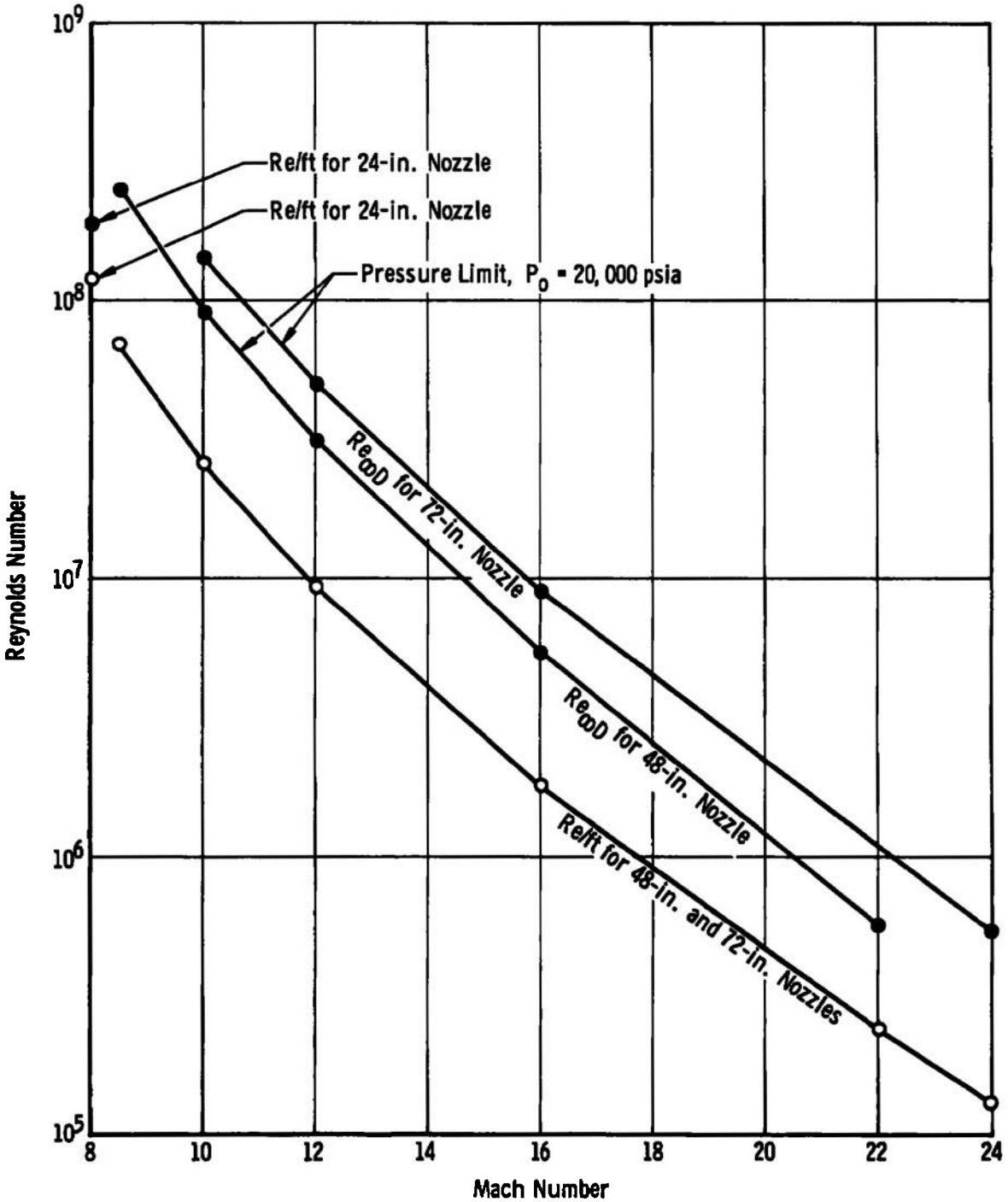

Figure 10. Maximum Reynolds number for the Cornell hypersonic shock tunnel (96-in. leg).

It should be noted here that under perfect gas simulation criteria, no extremely high and operationally unrealistic temperatures are encountered here, even for the maximum Reynolds number conditions. Since the tailored interface mode of operations permits operation at constant reservoir conditions, the maximum Reynolds number per foot performance for all nozzles falls along a single curve when plotted against Mach number. As with the case of Tunnel F which was considered in the last section, the advantage of a large nozzle is evident here when comparing on a $Re_{\infty D}$ basis.

3. VKF-AEDC TUNNEL C

An excellent example of the continuous type conventional, high Mach number test facility is Tunnel "C" of the von Karman Gas Dynamics Facility (VKF), Arnold Engineering Development Center (AEDC). This closed-circuit tunnel operates from the 92,500 horsepower VKF compressor system to provide continuous operation at Mach 10 and 12 in a 50-inch diameter test section using an axisymmetric contoured nozzle. Reservoir temperature of 1054°K for Mach 10 and 1305°K for Mach 12 are supplied by the combination of compressor heat of compression, a natural-gas-fired combustion heater, and electric resistance heaters. Due to its continuous operation, it is necessary that the entire tunnel be cooled by integral, external water jackets. Maximum reservoir pressures for Mach 10 and 12 operation (supplied by the VKF compressor system) are 1850 psi and 2000 psi respectively. The maximum Reynolds number operation parameters for Tunnel "C" are given in Table V, and are presented graphically in Figure 11.

TABLE V
MAXIMUM REYNOLDS NUMBER PERFORMANCE OF TUNNEL C

M_∞	P_o psia	T_o (1) °K	$\frac{Re/ft}{P_o}$ (1)	Re/ft	δ (2) ft.	$Re_{\infty D}$
10	1850	1054	1250	2.30×10^6	0.60	6.80×10^6
12	2000	1305	470	0.94×10^6	0.94	2.50×10^6

(1)This value obtained from Figure A-2a, page 73, of the Appendix.

(2)This value is obtained by using Equation 14, page 31.

4. THE VKI "LONGSHOT" FREE-PISTON TUNNEL

As a final example of performance predictions for high Mach number, high Reynolds number perfect gas test facilities, the "Longshot" free-piston tunnel (25, 26, 27) of the von Karman Institute for Fluid Dynamics (VKI), Rhode-Saint-Genese, Belgium, will now be considered. A free-piston tunnel is essentially a shock tunnel (as described in Section II of this chapter) with a solid interface (the piston) separating the driver gas from the driven (test) gas. The facility consists of a high pressure driver tube, an 89.5-foot barrel, a 6° half-angle conical nozzle with 24-inch exit diameter, and a combined test section and vacuum tank. The end of the barrel next to the nozzle is separated from the remainder of the barrel by a check-valve plate, thus forming a 19.4 cubic inch reservoir between the valve plate and the nozzle entrance. Prior to running, a 5 to 15 pound piston (held in place by an aluminum shear disc) separates the driver section at 5000 to 15,000 psia from the

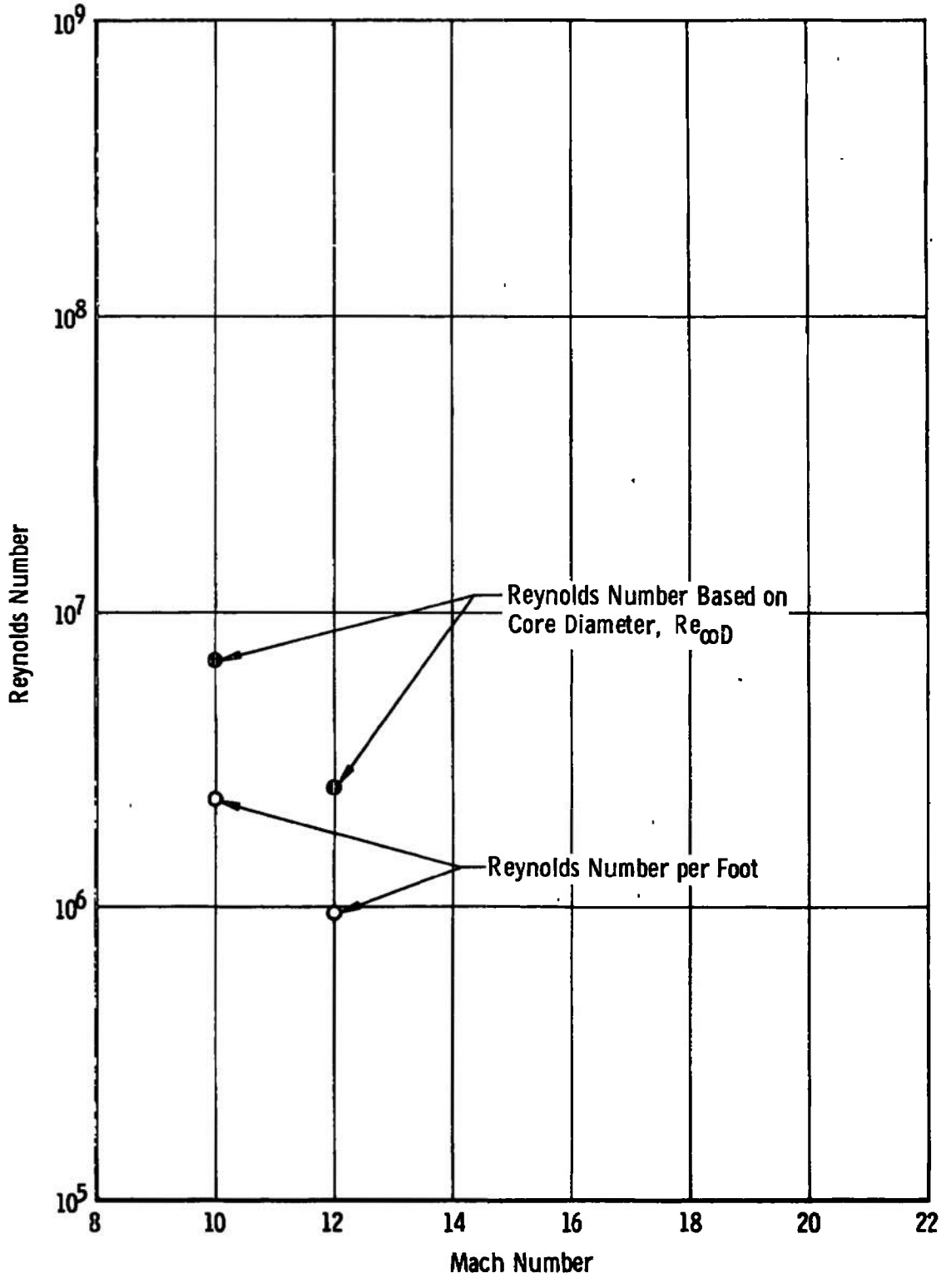

Figure 11. Maximum Reynolds number performance for the VKF-AEDC 50-in. diameter Tunnel C.

barrel section which is pressurized with nitrogen test gas at 50 to 200 psia. The nozzle and vacuum tank are separated from the reservoir by a diaphragm and are evacuated to low pressure. With sufficient overpressure the aluminum disc shears and the piston is accelerated down the barrel at speeds up to 2000 feet per second. The strong shock wave ahead of the piston heats and compresses the nitrogen which then flows subsonically through the check valves and into the reservoir. As the piston rebounds, the check valves close, trapping the nitrogen in the reservoir at maximum conditions of $P_o \cong 50{,}000$ psia and $T_o = 2500°K$. If the system of check valves was not used, the high pressure, high temperature conditions generated at the end of the barrel would rapidly decay. The test gas is subsequently expanded to Mach numbers of 15 to 27. Although in the present operation of this facility (25, 26) the test gas is allowed to expand to the condensation threshold, expansion only to the theoretical saturation temperature (see Figure 8, page 33) will be considered in this analysis. This restriction will hence limit the maximum Mach number to 18 as may be seen from Figure A-1e, page 69, of the Appendix.

As with the operation of Tunnel F which was considered in Section I of this chapter, the Longshot reservoir conditions are subject to decay with time. Unlike Tunnel F with its relatively large volume reservoir, the small 19.4 cubic inch reservoir of Longshot leads to relatively high decay rates, amounting to 5 per cent per millisecond at Mach 15 compared to 0.1 per cent per millisecond in the 54-inch test section of Tunnel F at Mach 15. Test times for Longshot are on the order of 10 milliseconds and useful data may be obtained two milliseconds after

the start of the run. Using the decay rates of Richards and Enkenhus (28), the test conditions for Longshot at t = 2 msec are given in Table VI, and presented graphically in Figure 12.

TABLE VI
MAXIMUM REYNOLDS NUMBER PERFORMANCE OF THE VKI LONGSHOT

M_∞	d^* in.	P_o psia	$\frac{Re/ft}{P_o}$ (1)	Re/ft	T_o (1) °K	δ (2) ft.	$Re_{\infty D}$
15	0.37	32,500	180	5.85×10^6	1850	0.27	8.6×10^6
18	0.25	40,000	52	2.08×10^6	2500	0.34	2.8×10^6
20	0.20	44,000	26	1.14×10^6	2850	0.39	1.4×10^6

(1)This value is obtained from Figure A-1e, page 69, of the Appendix.

(2)This value is obtained from Equation 14, page 31.

The operating range defined in Figure 12 is considerably reduced from that decribed by Richards and Enkenhus (26, 27) due to the restriction herein imposed that operation be limited to the theoretical saturation line of Figure 8, page 33.

5. SUMMARY OF COMPARISONS

The results of the four preceding analyses are summarized in Figure 13. Here it is evident that both large test section size and high reservoir pressure are the controlling parameters in attaining high Reynolds numbers. The restriction of continuous operation is evident

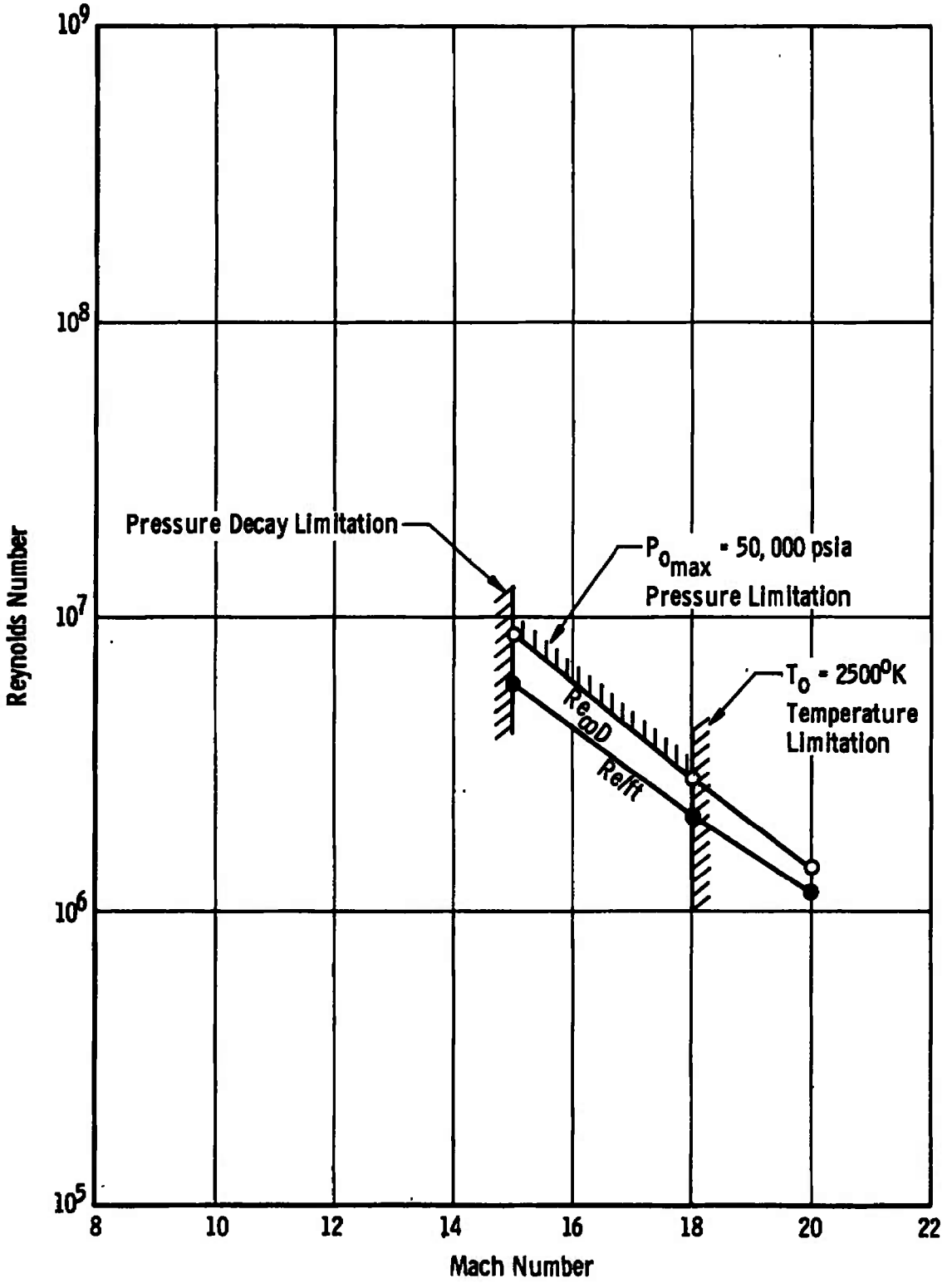

Figure 12. Maximum Reynolds number performance of the VKI "longshot".

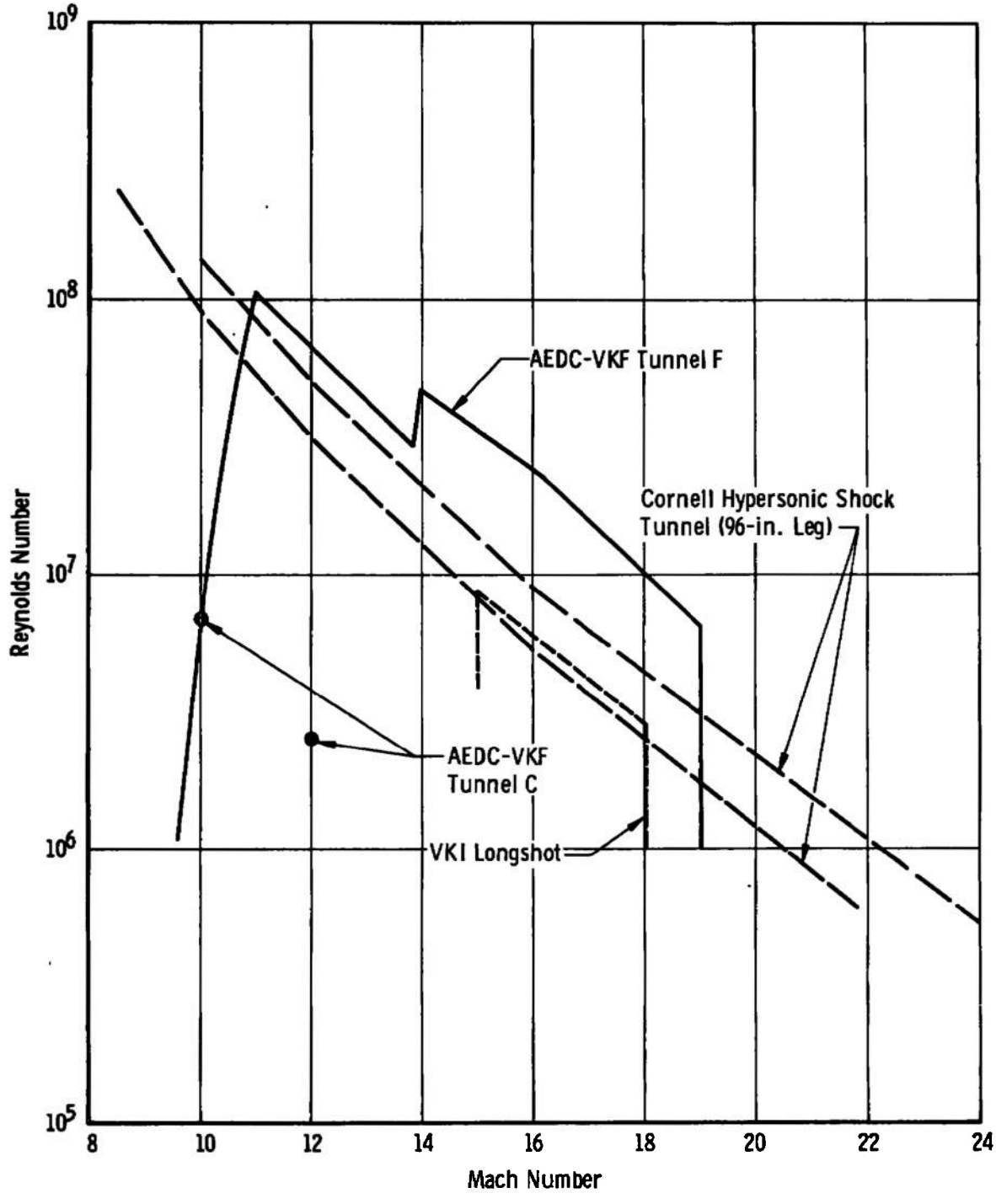

Figure 13. Comparison of high Reynolds number facilities.

when comparing Tunnel C with the other three facilities which are intermittent types. Figure 13 essentially represents the "state of the art" in high Mach number, high Reynolds number perfect gas test facilities.

SECTION V
CONCLUSION

Through an investigation of high velocity flight, four primary conclusions may be drawn:

1. Modern aerospace systems require simulation in the high velocity (high Mach number) regime.
2. At the altitudes of primary interest, high Reynolds number simulation is also required.
3. Thermo-chemical-kinetic effects in the flow about high velocity flight vehicles must be considered when discussing wind tunnel simulation.
4. The high Reynolds numbers required for adequate ground simulation cannot be produced in wind tunnels by testing at a lower Mach number than flight, except for certain relatively simple bodies for which the Mach number independence principle holds.

Real gas simulation is impractical in wind tunnels because it requires the duplication of stagnation enthalpy. Perfect gas simulation offers an alternative means of high velocity simulation and requires that only Mach number, Reynolds number, and the ratio of specific heats be duplicated. These requirements are within the scope of present technology, hence, there is a great deal of interest presently in perfect gas wind tunnels. There exists, therefore, a need to accurately predict and

compare the performance of perfect gas wind tunnel facilities.

The prediction or comparison of the performance of perfect gas wind tunnels operating at high Mach numbers and high Reynolds numbers should be based on the following six criteria:

1. All estimates of performance should be based on quoted operating ranges of the reservoir temperature and pressure (or the equivalent enthalpy and entropy).
2. Real gas expansions (such as those in the Appendix) should be used to determine unit Reynolds number over the quoted Mach number, reservoir pressure, and reservoir temperature range.
3. The reservoir test gas should be expanded to the saturation temperature as given in Figure 8, page 33.
4. The viscosity used in the calculation of Reynolds number should be obtained by using a linear relation for viscosity below 100°K (Equation 15, page 34) and the Sutherland viscosity formula (Equation 16, page 35) above 100°K.
5. The length term in the Reynolds number equation (Equation 6, page 26) should be taken as the experimentally determined core diameter, or a calculated core diameter using Equation 14, page 31, and geometric dimensions.
6. Since high Reynolds number conditions are to be compared, non-equilibrium effects should be assumed negligible.

BIBLIOGRAPHY

1. Korkegi, Robert H., Roshi Kubota, and F. E. Mickey. "Survey and Analysis of Hypersonic Testing," University of Southern California Engineering Center Report No. 62-101, Los Angeles, California, October, 1957.

2. Probstein, R. F. "Shock Wave and Flow Field Development in Hypersonic Reentry," American Rocket Society Journal, 31:185-194, February, 1961.

3. Harney, Donald J. "Chemical Kinetic Regimes of Hypersonic Flight Simulation," Arnold Engineering Development Center TDR-63-3, Arnold Air Force Station, Tennessee, January, 1963.

4. Griffith, B. J., and D. E. Boylan. "Reynolds and Mach Number Simulation of Apollo and Gemini Reentry and Comparisons with Flight," Advisory Group for Aerospace Research and Development, North Atlantic Treaty Organization, Conference Proceedings No. 30, 7 Rue Ancelle 92, Neuilly-Sur-Seine, France, May, 1968.

5. Cassanto, J. M., N. S. Rasmussen, and J. D. Coats. "Correlation of Measured Free Flight Base Pressure Data for M = 4 to M = 19 In Laminar and Turbulent Flow," American Institute of Aeronautics and Astronautics Paper No. 68-699, June, 1968.

6. Lukasiewicz, J. "Atmospheric Entry Test Facilities: Limitations of Current Techniques and Proposal for a New Type Facility," American Institute of Aeronautics and Astronautics Paper No. 69-166, January, 1969.

7. Potter, J. L. "Hypersonic Flight Simulation: Aerodynamics," Paper presented at the Conference on the Role of Simulation in Space Technology, Virginia Polytechnic Institute, Blacksburg, Virginia, August, 1964.

8. Gregorek, G. M., and S. L. Petrie. "A Variable Atmosphere Hypersonic Wind Tunnel for Similitude Studies," Air Force Flight Dynamics Laboratory TR-66-96, Wright-Patterson Air Force Base, Ohio, September, 1966.

9. Whitfield, J. D., and J. L. Potter. "Simulating High-Speed Aerodynamics," Space/Aeronautics, 47:83-91, March, 1967.

10. Charwat, A. F. "A Generalized Analysis of the Performance Characteristics and Operating Ranges of Hypervelocity-Flow Test Facilities," Rand Report R-432-PR, Rand Corporation, Santa Monica, California, January, 1965.

11. Whitfield, Jack D., and Glenn D. Norfleet. "Source Flow Effects in Conical Hypervelocity Nozzles," Arnold Engineering Development Center TDR-62-116, Arnold Air Force Station, Tennessee, June, 1969.

12. Osgerby, I. T., and H. K. Smithson. "Operation of AEDC-VKF 100 In. Hotshot Tunnel F with Air as a Test Gas and Application to Scramjet Testing," Arnold Engineering Development Center TR-67-242, Arnold Air Force Station, Tennessee, December, 1967.

13. Edenfield, Emmett E., Jr. "Contoured Nozzle Design for Hotshot Wind Tunnels," Unpublished Masters thesis, The University of Tennessee, Knoxville, 1967.

14. Daum, Fred L., and George Gyarmthy. "Condensation of Air and Nitrogen In Hypersonic Wind Tunnels," AIAA Journal, 6:458-465, March, 1968.

15. Hilsenrath, Joseph, et al. Tables of Thermal Properties of Gases. National Bureau of Standards Circular 564, United States Department of Commerce. Washington: Government Printing Office, 1955.

16. Yos, Jerrold M. "Transport Properties of Nitrogen, Hydrogen, Oxygen, and Air to 30,000°K," AVCO Corporation RAD-TM-63-7, Everett, Massachusetts, March, 1963.

17. Bromley, L. A., and C. R. Wilke. "Viscosity Behavior of Gases," Industrial and Engineering Chemistry, 43:1641-1648, July, 1951.

18. Fiore, Anthony W. "Viscosity of Air," Journal of Spacecraft, 3:756-758, May, 1966.

19. Neel, C. A., and C. H. Lewis. "Interpolations of Imperfect Nitrogen Thermodynamic Data at Constant Entropy," Arnold Engineering Development Center TDR-64-212, Arnold Air Force Station, Tennessee, October, 1964.

20. Neel, C. A., and Clark H. Lewis. "Interpolations of Imperfect Air Thermodynamic Data at Constant Entropy," Arnold Engineering Development Center TDR-63-183, Arnold Air Force Station, Tennessee, September, 1964.

21. Cornell Aeronautical Laboratory Hypersonic Shock Tunnel, Description and Capabilities. Cornell University, Buffalo, New York, 1968.

22. Hertzberg, A., C. E. Wittliff, and J. G. Hall. "Development of the Shock Tunnel and Its Application to Hypersonic Flight," Hypersonic Flow Research. New York: Academic Press, 1962. Pp. 701-758.

23. Ferri, Antonio. "Hypersonic Flight Testing," International Science and Technology, 28:64-76, April, 1964.

24. Nagamatsu, H. T. "Shock Tube Technology and Design," Fundamental Data Obtained from Shock-Tube Experiments. New York: Pergamon Press, 1961. Pp. 86-136.

25. Richards, B. E., and K. R. Enkenhus. "Hypersonic Testing in the VKI Longshot Free-Piston Tunnel," American Institute of Aeronautics and Astronautics Paper No. 69-333, April, 1969.

26. Richards, B. E., and K. R. Enkenhus. "The Longshot Free Piston Hypersonic Tunnel," von Karman Institute for Fluid Dynamics TN-49, Rhode-Saint-Genese, Belgium, September, 1968.

27. Boison, J. Christopher. "Longshot I Hypersonic Free Piston Tunnel," Republic Aviation Corporation Report 1884A, Farmingdale, Long Island, New York, December, 1963 (Revised May, 1965).

APPENDIX
REAL GAS EXPANSIONS

Real gas nitrogen and air expansions are presented in Figures A-1 and A-2. These data are based upon previously unpublished computer solutions by Emmett E. Edenfield of the Aerodynamics Section, Hypervelocity Branch, von Karman Gas Dynamics Facility, Arnold Engineering Development Center.

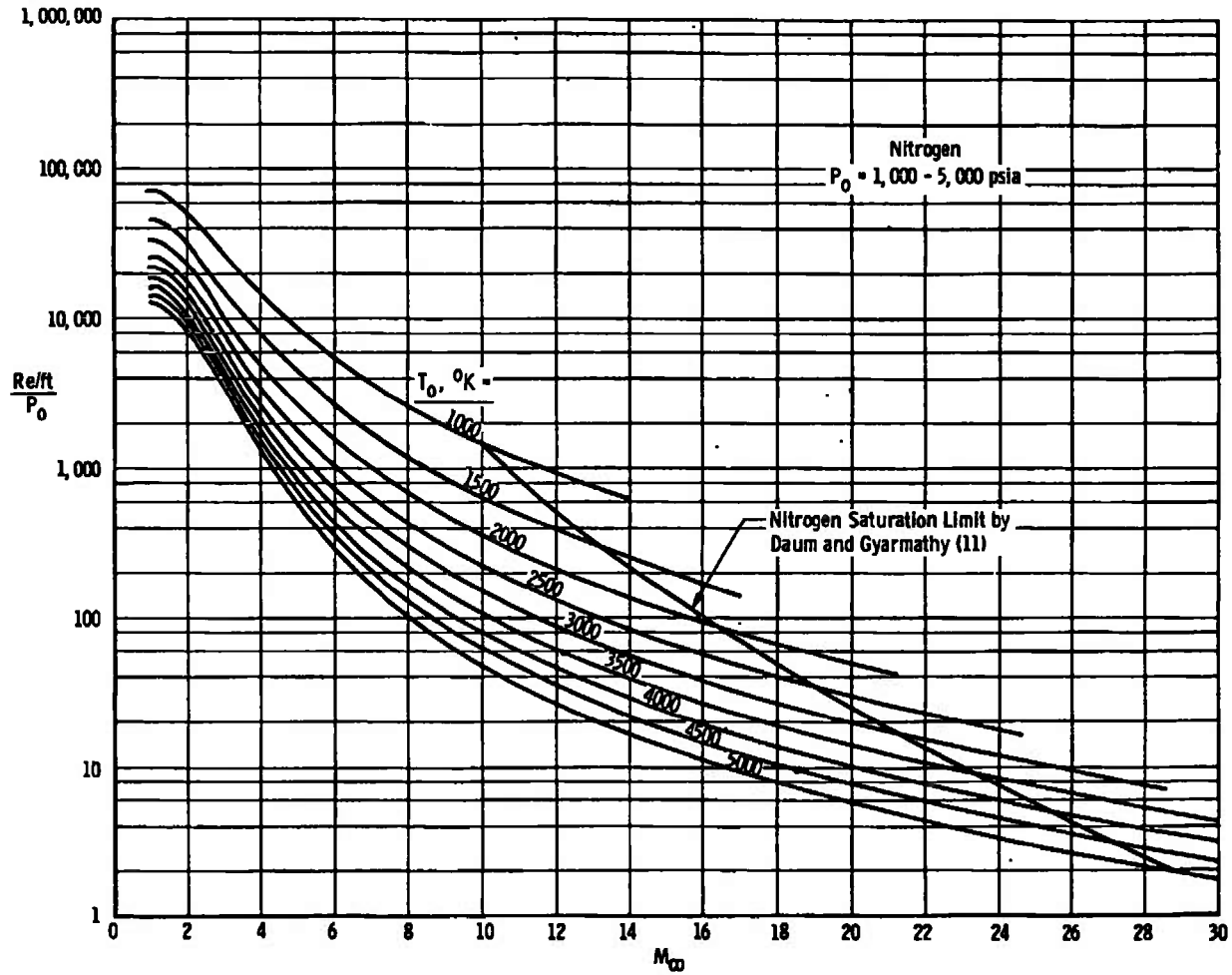

a. P_o = 1000-5000 psia.

Figure A-1. Mach number-unit Reynolds number relations for real gas nitrogen expansions.

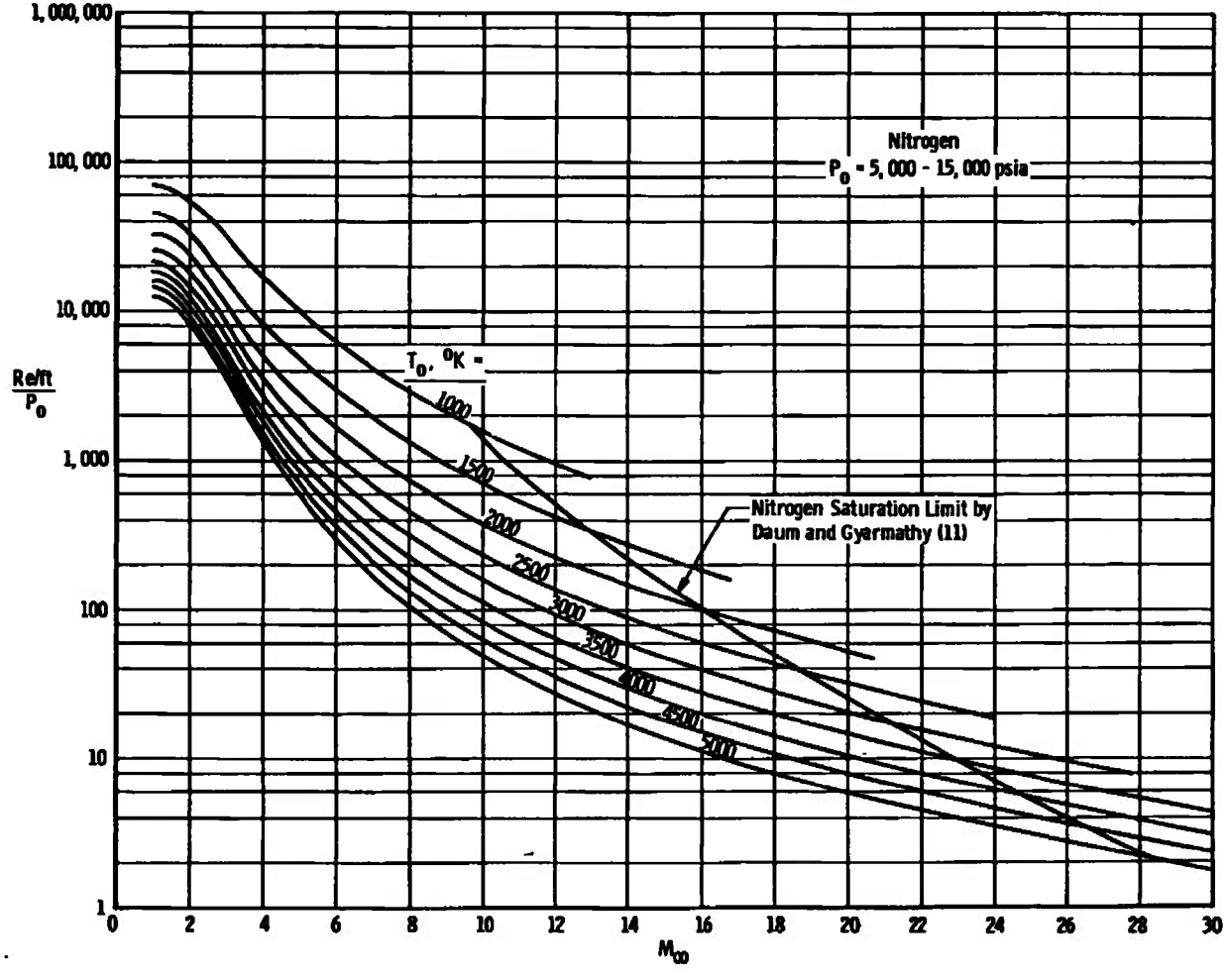

b. P_o = 5000-15,000 psia.

Figure A-1. (continued)

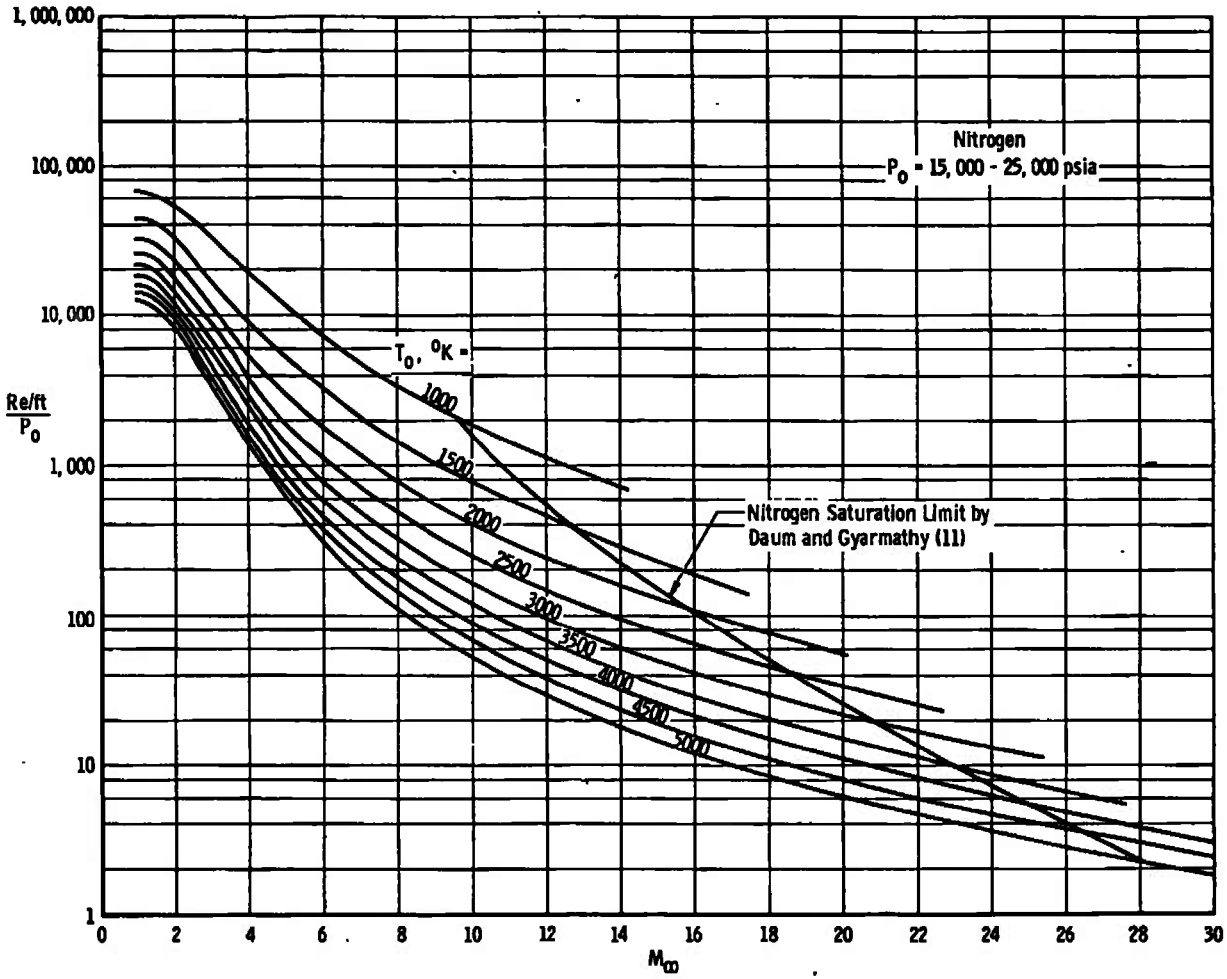

c. P_o = 15,000-25,000 psia.

Figure A-1. (continued)

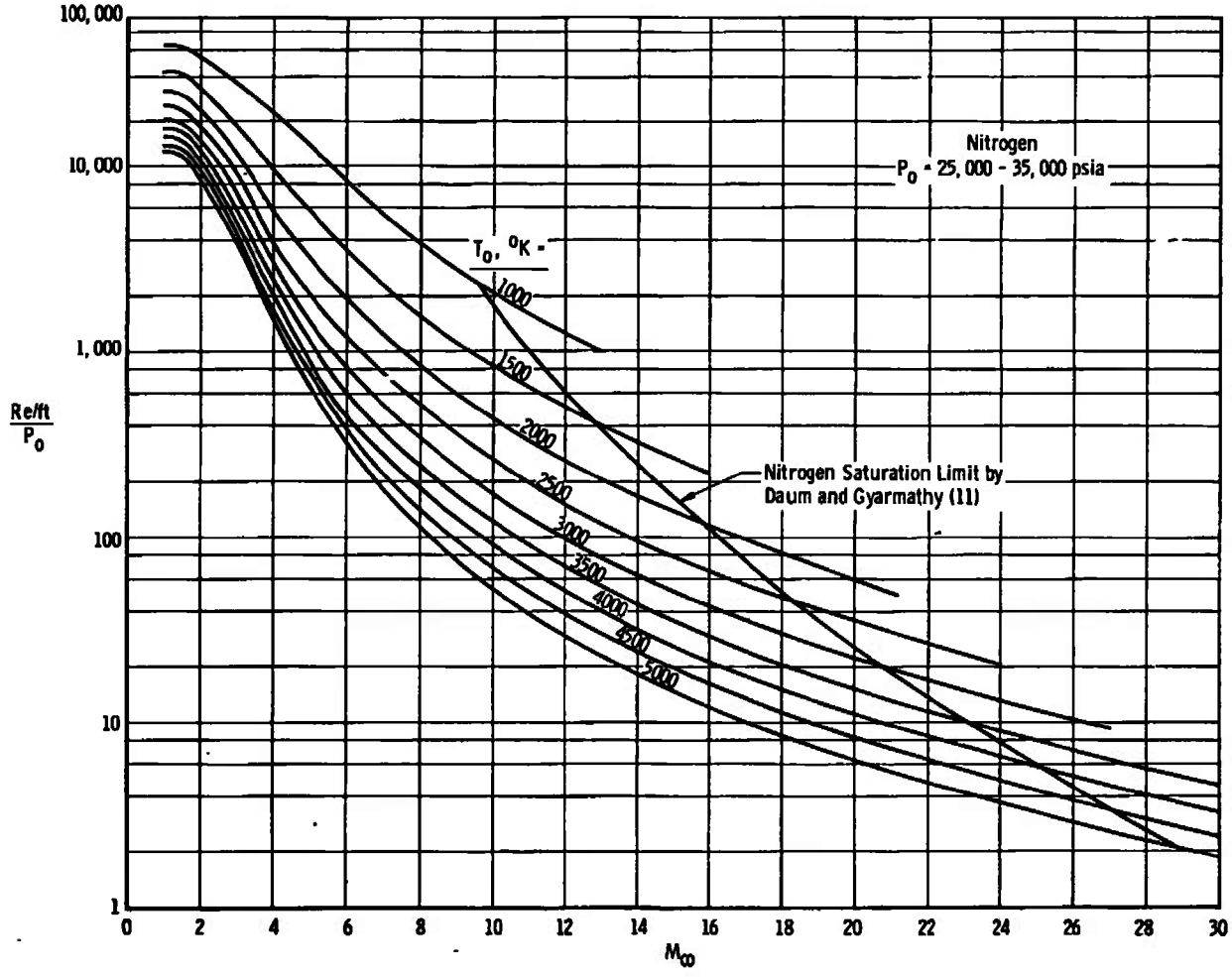

d. P_o = 25,000-35,000 psia.

Figure A-1. (continued)

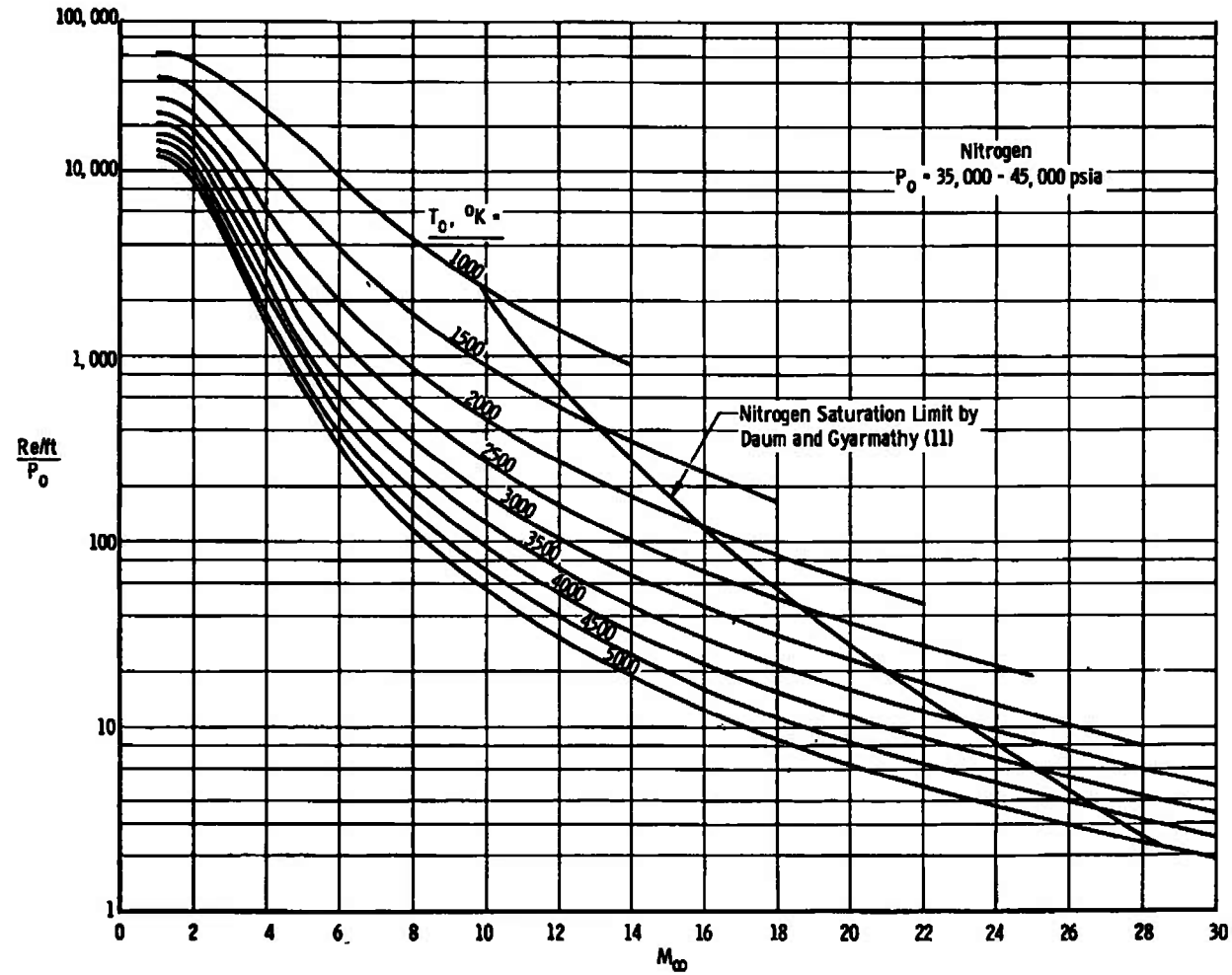

e. P_o = 35,000-45,000 psia.

Figure A-1. (continued)

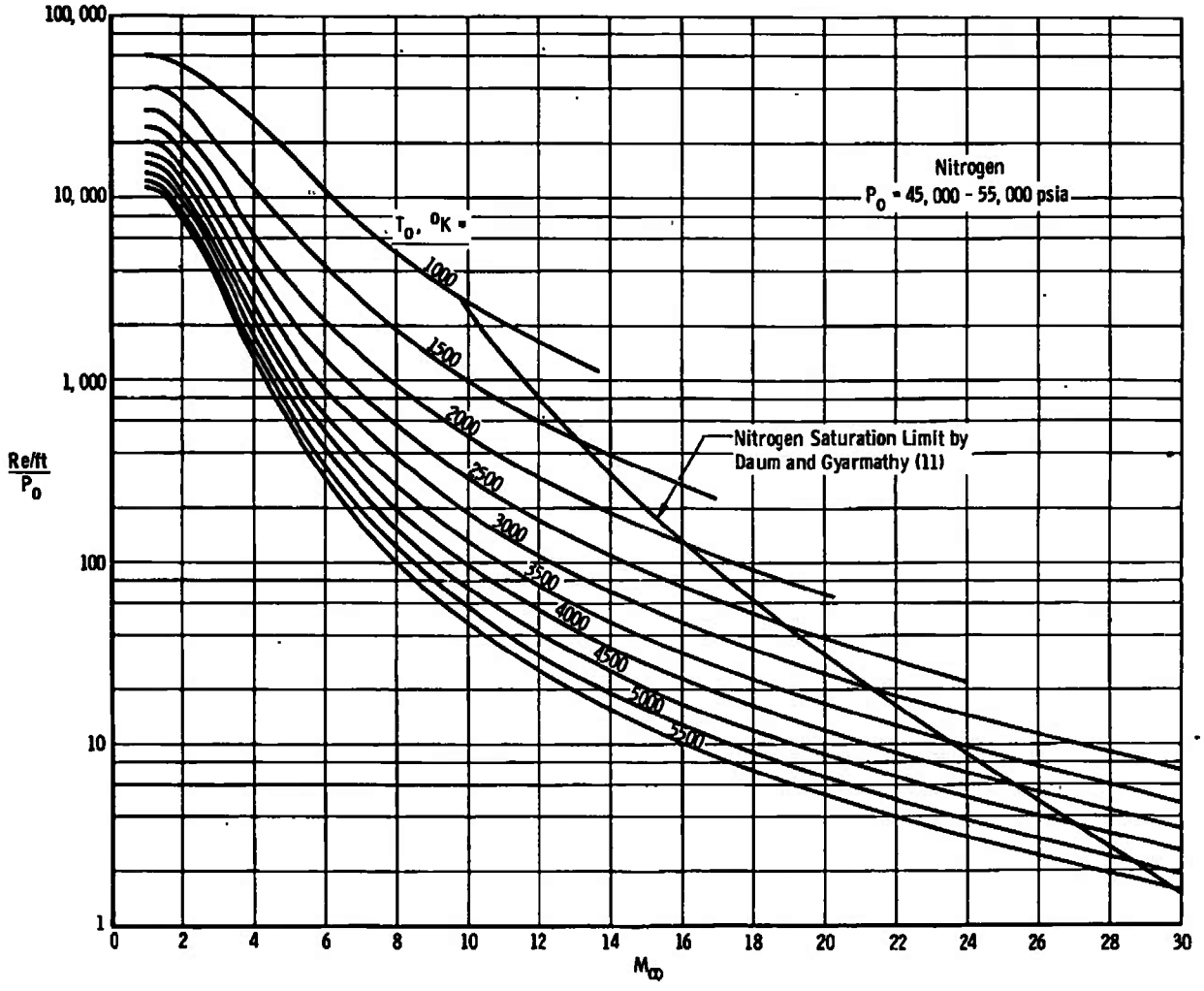

f. P_o = 45,000-55,000 psia.

Figure A-1. (continued)

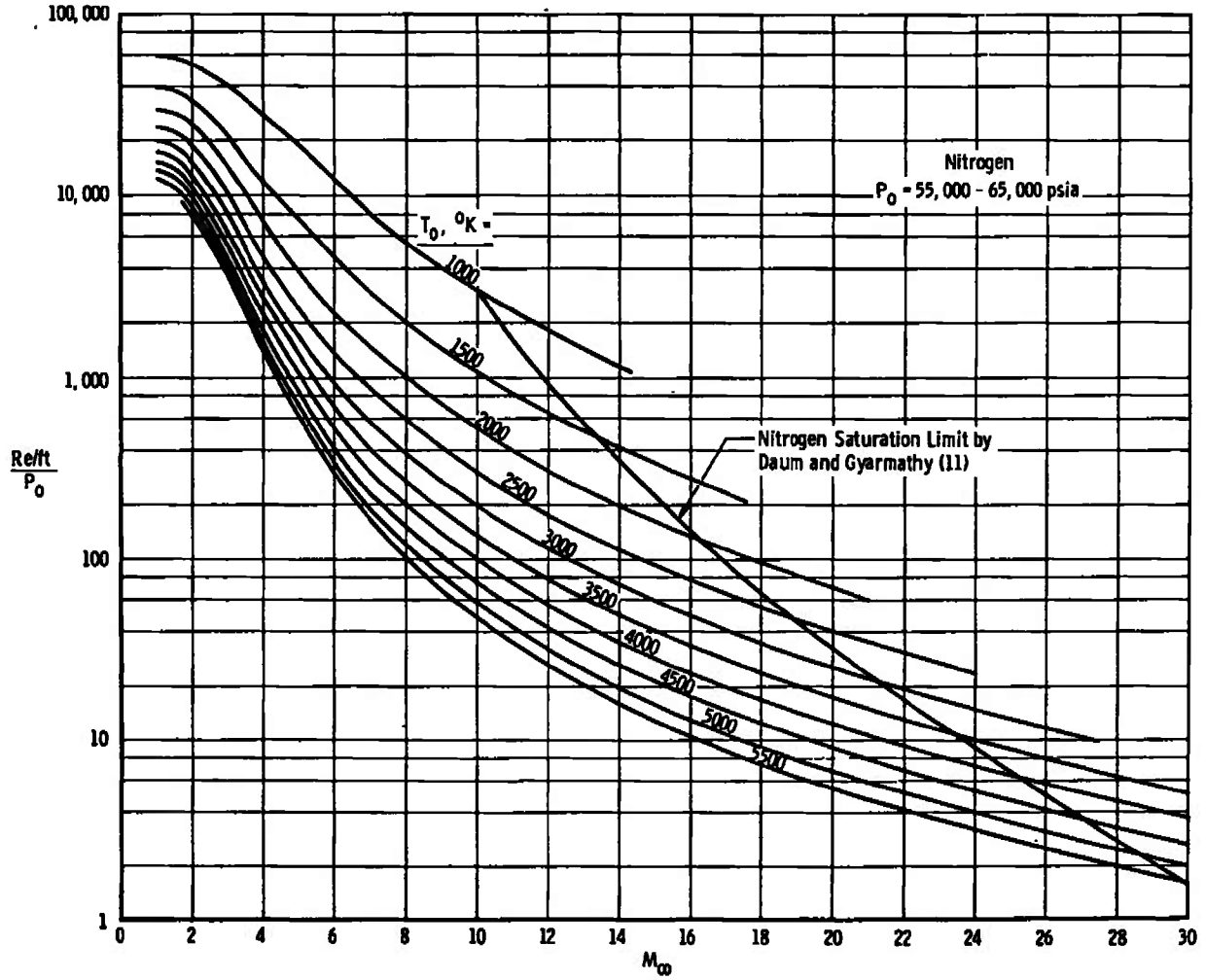

g. P_o = 55,000-65,000 psia.

Figure A-1. (continued)

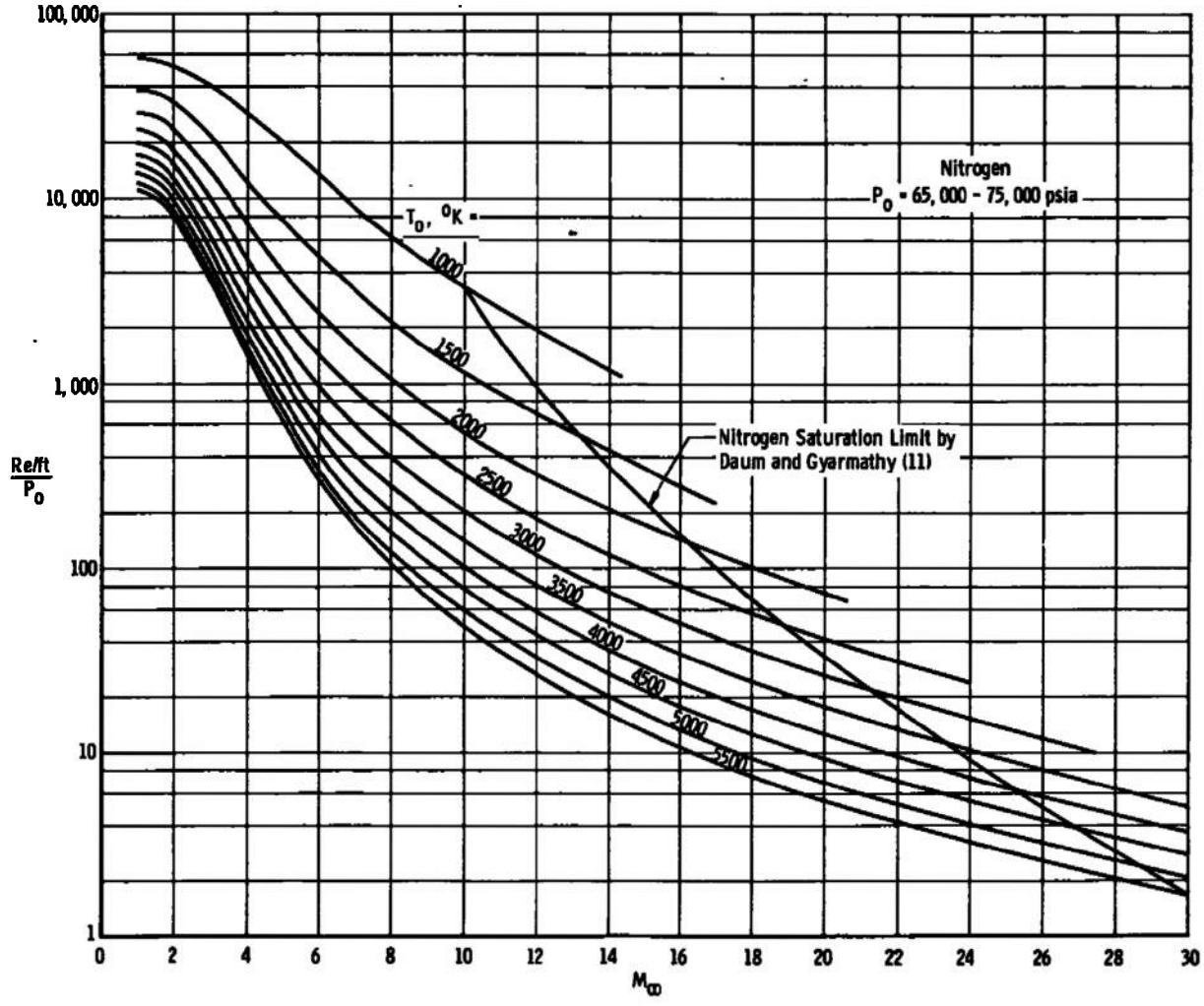

h. P_o = 65,000-75,000 psia.

Figure A-1. (continued)

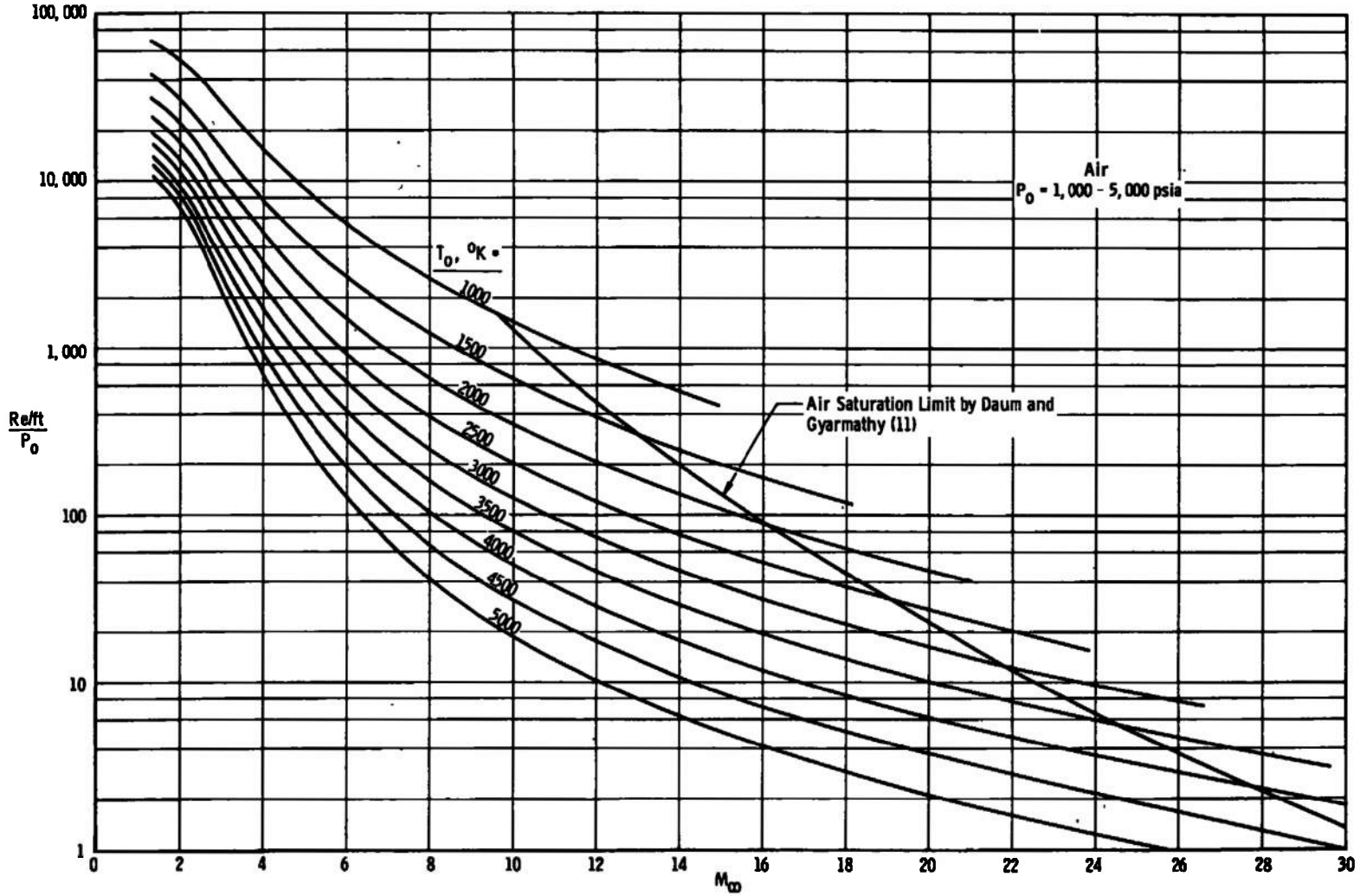

a. P_o = 1000-5000 psia.

Figure A-2. Mach number-unit Reynolds number relations for real gas air expansions.

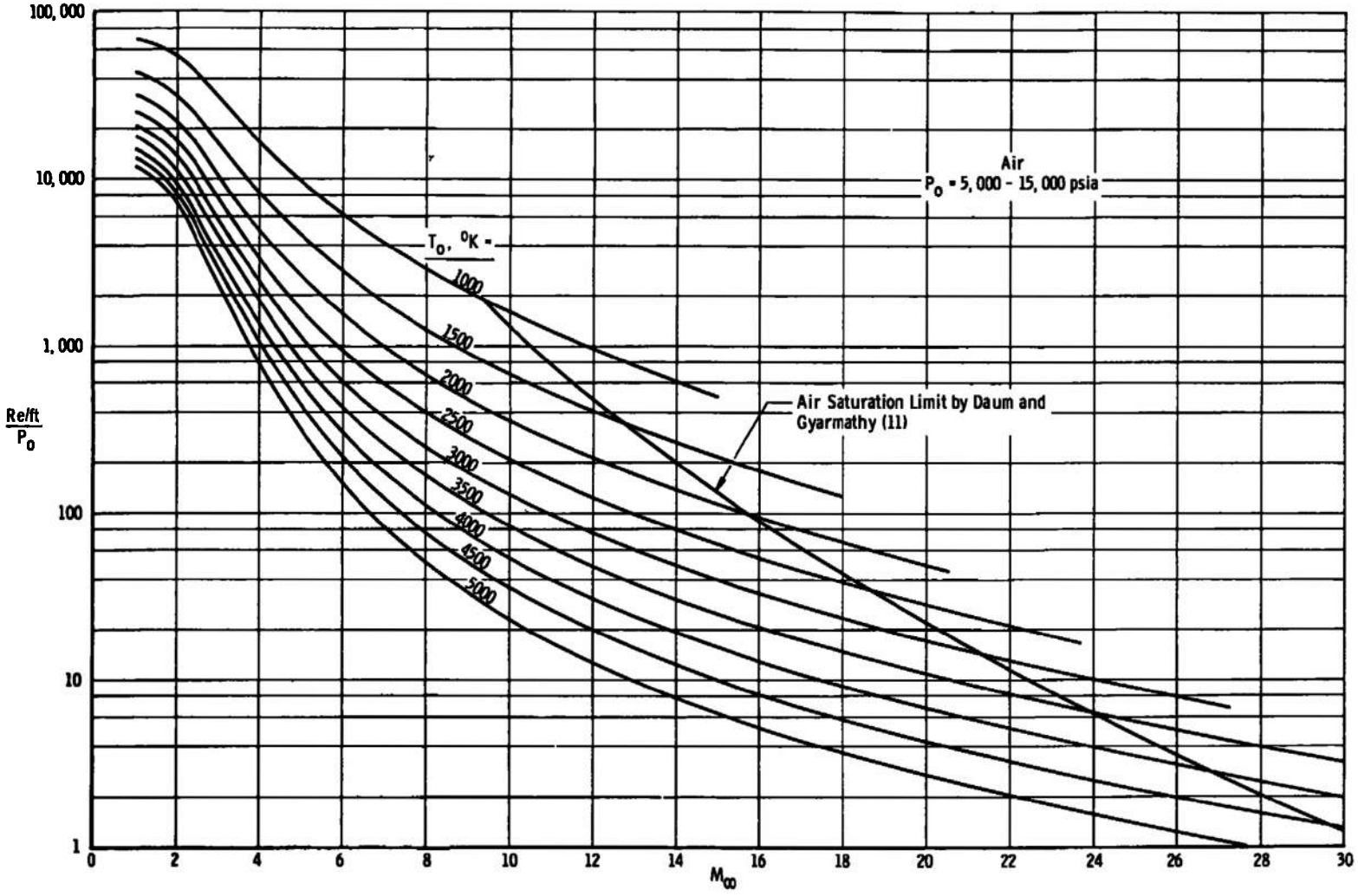

b. P_o = 5000-15,000 psia.

Figure A-2. (continued)

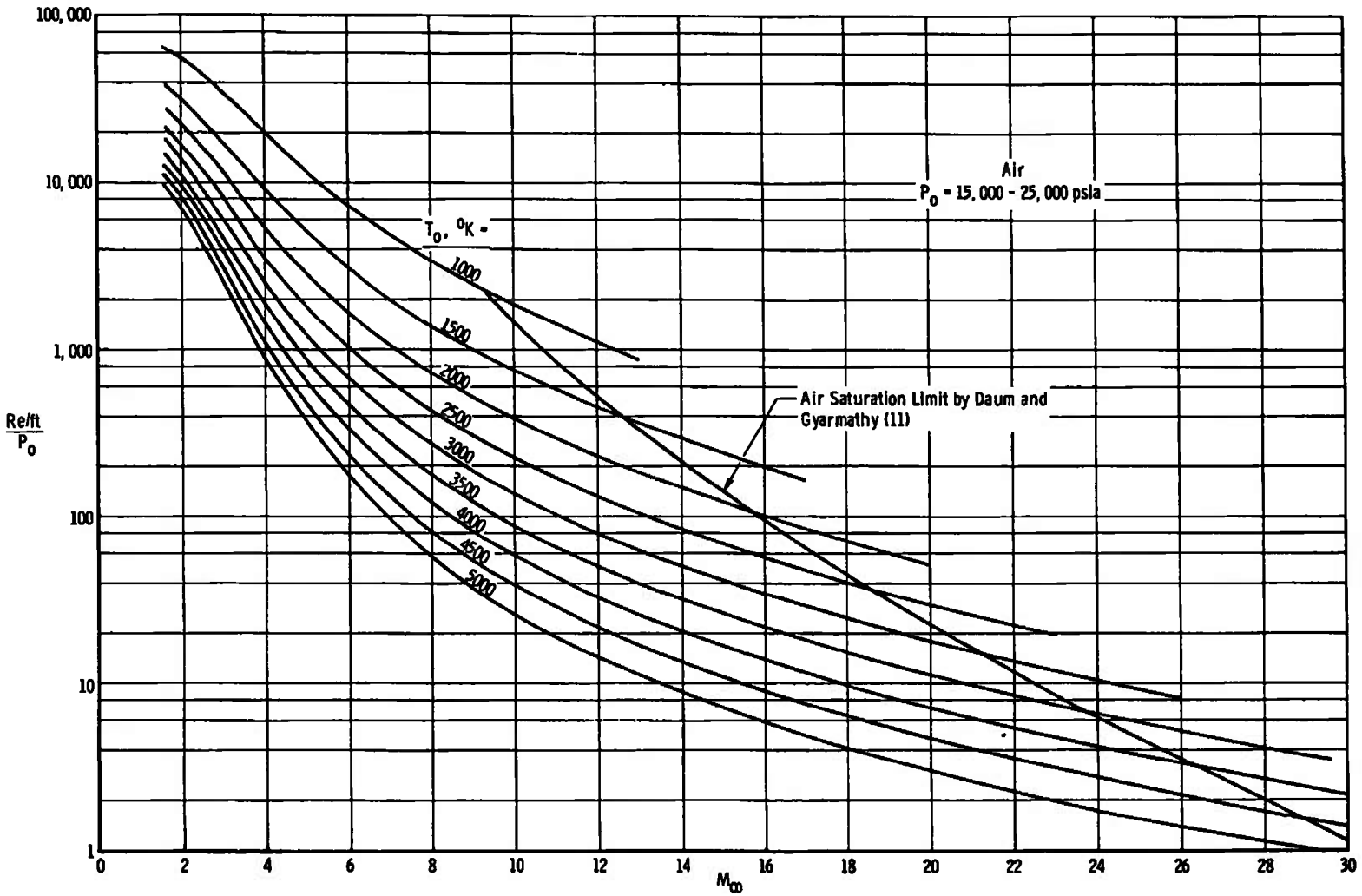

c. P_o = 15,000-25,000 psia.

Figure A-2. (continued)

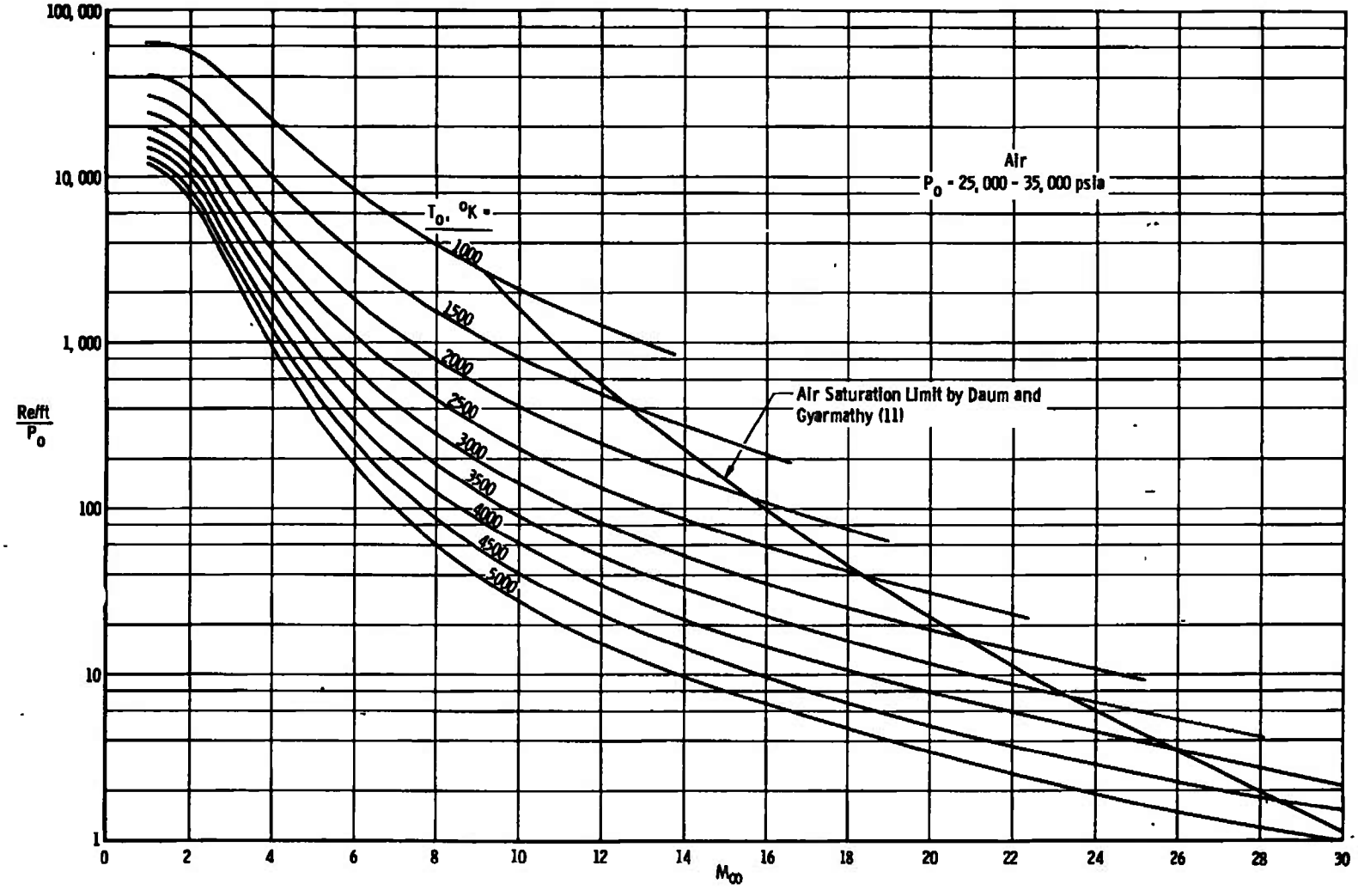

d. P_O = 25,000-35,000 psia.

Figure A-2. (continued)

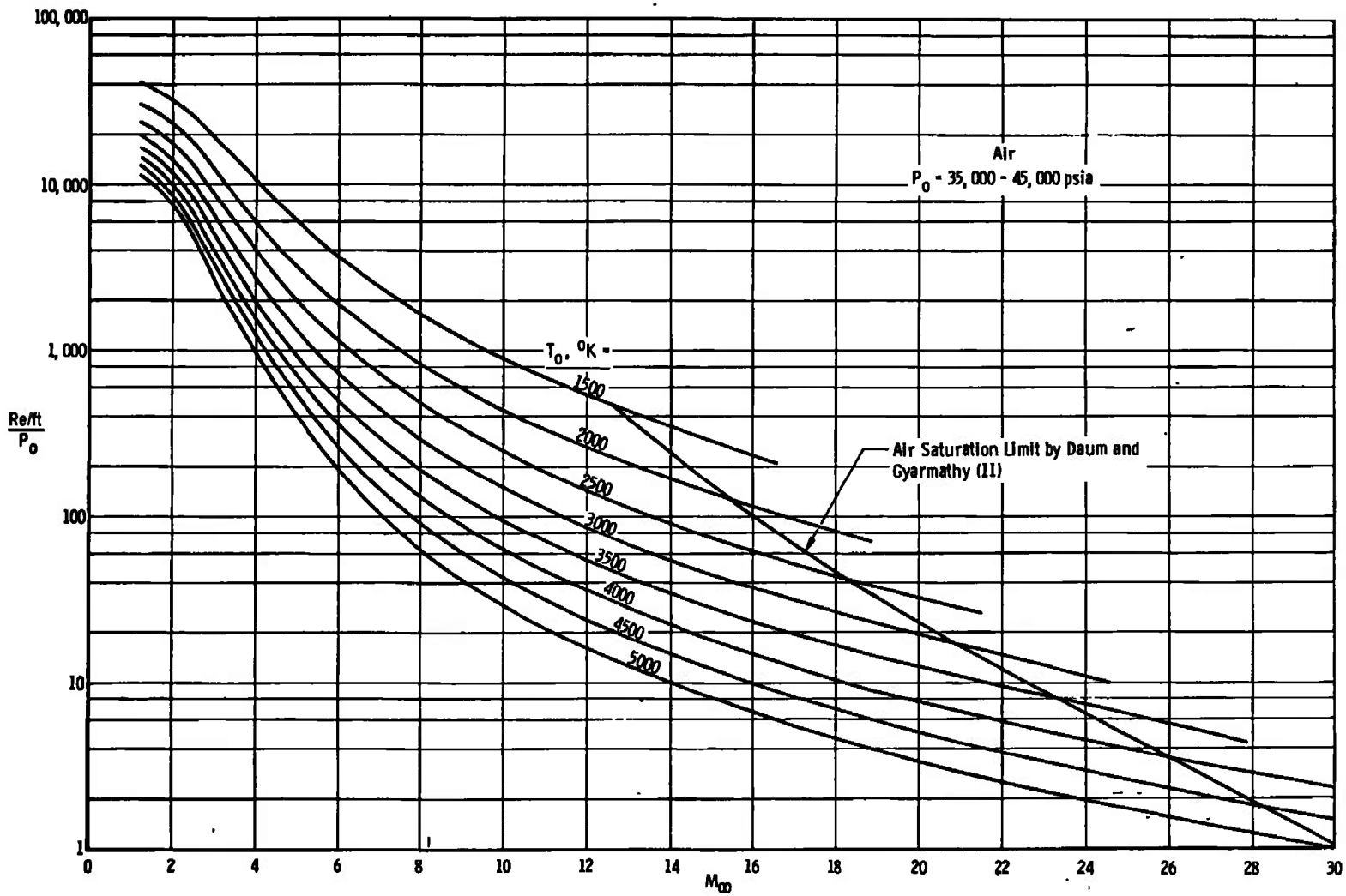

e. P_0 = 35,000-45,000 psia.

Figure A-2. (continued)

UNCLASSIFIED

Security Classification

DOCUMENT CONTROL DATA - R & D

(Security classification of title, body of abstract and indexing annotation must be entered when the overall report is classified)

1. ORIGINATING ACTIVITY (Corporate author)	2a. REPORT SECURITY CLASSIFICATION
Arnold Engineering Development Center ARO, Inc., Operating Contractor Arnold Air Force Station, Tennessee 37389	UNCLASSIFIED
	2b. GROUP N/A

3. REPORT TITLE

HIGH MACH NUMBER, HIGH REYNOLDS NUMBER PERFECT GAS WIND TUNNELS, AND A METHOD OF PERFORMANCE COMPARISON

4. DESCRIPTIVE NOTES (Type of report and inclusive dates)

May 5 to July 15, 1969 - Final Report

5. AUTHOR(S) (First name, middle initial, last name)

A. H. Boudreau, Jr., ARO, Inc.

This document has been approved for public release . . . its distribution is unlimited. per A.F. Letter dated Jan. '73 signed William D. Cole

6. REPORT DATE	7a. TOTAL NO. OF PAGES	7b. NO. OF REFS
January 1970	87	27

8a. CONTRACT OR GRANT NO.	9a. ORIGINATOR'S REPORT NUMBER(S)
F40600-69-C-0001	
b. PROJECT NO.	AEDC-TR-69-268
c. Program Element 65401F/876/G226	9b. OTHER REPORT NO(S) (Any other numbers that may be assigned this report)
d.	N/A

10. DISTRIBUTION STATEMENT This document is subject to special export controls and each transmittal to foreign governments or foreign nationals may be made only with prior approval of Arnold Engineering Development Center (AETS), Arnold Air Force Station, Tennessee 37389.

11. SUPPLEMENTARY NOTES	12. SPONSORING MILITARY ACTIVITY
Available in DDC	Arnold Engineering Development Center, Air Force Systems Command, Arnold AF Station, Tenn. 37389

13. ABSTRACT

The regimes of high velocity flight are investigated and simulation of such conditions is shown to require simulation of high Reynolds numbers in addition to high Mach numbers, plus consideration of thermo-chemical-kinetic effects. Real gas simulation, which requires duplication of stagnation enthalpy is shown to be impractical in wind tunnels. Perfect gas simulation is, however, shown to offer an alternative means of high velocity simulation. Considerations of perfect gas simulation are discussed which include non-equilibrium of the test gas, source flow considerations, and saturation limits. A method of comparing perfect gas wind tunnels is then developed based on the basic fluid dynamics scaling parameters plus considerations of reservoir pressure limits and decay rates, wind tunnel size, saturation temperature limits, viscosity considerations, and nitrogen as a test gas. Computer calculations of real gas air and nitrogen expansions for unit Reynolds number are presented graphically based on the method developed for comparing facilities. Finally, four perfect gas wind tunnel facilities which represent the present state of the art are compared using the developed technique.

This document is subject to special export controls and each transmittal to foreign governments or foreign nationals may be made only with prior approval of Arnold Engineering Development Center (AETS), Arnold Air Force Station, Tennessee 37389.

DD FORM 1 NOV 65 1473

UNCLASSIFIED

Security Classification

14. KEY WORDS	LINK A ROLE	LINK A WT	LINK B ROLE	LINK B WT	LINK C ROLE	LINK C WT
wind tunnels						
performance						
perfect gas simulation						
high Reynolds number wind tunnels						
high Mach number wind tunnels						
fluid dynamics						

1. Perfect gas wind tunnels

4. Shock Tunnels -- Performance

5 Hypersonic wind tunnels -- "

17-3

AFSC
Arnold AFS Tenn